

## Phase transitions in the Earth's mantle and mantle mineralogy

YINGWEI FEI and CONSTANCE M. BERTKA

Geophysical Laboratory, Carnegie Institution of Washington, 5251 Broad Branch Road, N.W.,  
Washington, DC 20015, U.S.A.

**Abstract**—High-pressure and high-temperature experiments on mantle minerals and rocks have provided basic knowledge for the understanding of the mineralogical constitution of the Earth's mantle. It is generally understood that the Earth's upper mantle consists of olivine, orthopyroxene, clinopyroxene, and garnet. The olivine-wadsleyite ( $\alpha$ - $\beta$ ) transition at about 13.5 GPa marks the beginning of the transition zone. At upper mantle and transition zone pressures, the pyroxene component gradually dissolves into the garnet structure, resulting in the completion of the pyroxene-majorite transformation at about 15.5 GPa. High CaO content in majorite is energetically unfavorable at high pressure, leading to the formation of  $\text{CaSiO}_3$  perovskite at pressures greater than 20 GPa. The sharp transformation from silicate spinel to ferromagnesian silicate perovskite and magnesiowüstite at about 24 GPa divides the lower mantle from the transition zone. Because most of the  $\text{Al}_2\text{O}_3$  resides in majorite at transition zone pressures, the transformation from majorite to an Al-bearing orthorhombic perovskite completes at a pressure higher than that of the postspinel transformation. The lower mantle consists of orthorhombic perovskite, magnesiowüstite, and  $\text{CaSiO}_3$  perovskite for a pyrolite model. As part of the mantle system, mid-ocean ridge basalt (MORB) generated at the mid-ocean ridge and subducted in the subduction zone. Phase transformations in basalt play an important role in mantle dynamics, particularly related to the subducted slab. Because basalt has high Al and Si content, the transformation to a perovskite lithology in basalt occurs at about 27 GPa, with an assemblage of Al-bearing orthorhombic perovskite,  $\text{CaSiO}_3$  perovskite, stishovite, and Al-phase.

### INTRODUCTION

IT HAS long been recognized that high-pressure phase transformations in the rock-forming minerals, particularly in olivine, may be correlated to the observed seismic velocity discontinuities in the Earth's mantle (e.g., BERNAL, 1936; BIRCH, 1952; RINGWOOD, 1958). A definitive proof for such correlations has to rely on experimental results on minerals such as olivine, pyroxene, and garnet, at high pressures and temperatures. Prior to 1966, simultaneous high-pressure and high-temperature experiments were limited to a maximum pressure of about 10 GPa, corresponding to a depth of about 300 km in the Earth's mantle. Therefore, the physical conditions of the transition zone, starting at a depth of 400 km, were not able to be simulated in the laboratory. Phase transformations in the Mg-rich region of  $(\text{Mg,Fe})_2\text{SiO}_4$  olivine, a predominant phase in the upper mantle, could not be directly observed at high pressures. However, experimental results on olivine-spinel transformations in analog systems such as germanates and Ni-, Co-, and Fe-olivines strongly suggested that phase transformation in  $\text{Mg}_2\text{SiO}_4$  olivine should occur at about 13 GPa (e.g., RINGWOOD and SEABROOK, 1962). In 1966, technical breakthrough in achieving higher pressures at high temperature finally made it possible to synthesize high-pressure polymorphs of  $\text{Mg}_2\text{SiO}_4$  (RINGWOOD and MAJOR, 1966; AKIMOTO and IIDA, 1966). Since then, numerous experiments have been conducted in the system  $\text{Mg}_2\text{SiO}_4$ - $\text{Fe}_2\text{SiO}_4$  to refine the

olivine-wadsleyite-spinel ( $\alpha$ - $\beta$ - $\gamma$ ) transition boundaries (e.g., RINGWOOD and MAJOR, 1970; SUIITO, 1972, 1977; KAWADA, 1977; OHTANI, 1979; FUKIZAWA, 1982; SAWAMOTO, 1986; KATSURA and ITO, 1989; MORISHIMA *et al.*, 1994), including new reversal experimental data on the  $\alpha$ - $\beta$  transition in the system  $\text{Mg}_2\text{SiO}_4$ - $\text{Fe}_2\text{SiO}_4$  presented in this paper. It is generally believed that the  $\alpha$ - $\beta$  transition is, at least partially, responsible for the observed 410-km seismic velocity discontinuity in the mantle. The remaining arguments on the nature of the 410-km discontinuity are more or less centered on the details of the match between high-pressure data and the seismic observations. The olivine fraction of the mantle (LI *et al.*, 1998; ZHA *et al.*, 1997, 1998) and the sharpness of the transition (e.g., FEI and BERTKA, 1996; STIXRUDE, 1997; IRIFUNE and ISSHIKI, 1998) are two examples of such arguments.

The 660-km discontinuity divides the mantle between the transition zone and the lower mantle. It was suggested that dissociation of ferromagnesian silicate spinel at pressures greater than 20 GPa may be responsible for this discontinuity (e.g., RINGWOOD, 1962b). The ultimate proof of the dissociation of spinel to a denser mineral assemblage came from the synthesis of orthorhombic ferromagnesian silicate perovskite in a laser-heated diamond-anvil cell (LIU, 1974, 1975, 1976). Subsequently, the phase relations in the systems  $\text{Mg}_2\text{SiO}_4$ - $\text{Fe}_2\text{SiO}_4$  and  $\text{MgSiO}_3$ - $\text{FeSiO}_3$  were studied at pressures between 15 and 70

GPa using the laser-heated diamond-anvil cell technique (YAGI *et al.*, 1979). The postspinel transformation boundaries in the Mg-rich region of the system  $\text{Mg}_2\text{SiO}_4\text{-Fe}_2\text{SiO}_4$  were further refined using a multi-anvil high-pressure apparatus (ITO and TAKAHASHI, 1989).

Driven by questions concerning the nature of the seismic velocity discontinuities and the mineralogical constitution of the Earth's mantle, experimentalists have developed and improved various high-pressure devices to simulate the pressure-temperature conditions in the deep interior of the Earth, notably the piston-cylinder apparatus and the multi-anvil device for mantle phase equilibrium study, and the diamond-anvil cell for measurements of physical properties of mantle minerals at high pressures. Pressures up to 27 GPa (corresponding to about 750 km in depth) can be routinely achieved in the multi-anvil apparatus with accurate temperature measurements up to 2500°C (*e.g.*, ITO and KATSURA, 1992; BERTKA and FEI, 1997; HIROSE *et al.*, 1999). A large database on phase equilibria for mantle minerals and model mantle composition systems has been accumulated over the last four decades. In this paper, we briefly review the high-pressure techniques commonly used for phase equilibrium study and summarize high-pressure experimental results in chemical systems related to the mantle, including  $\text{SiO}_2$ ,  $\text{Mg}_2\text{SiO}_4$ ,  $\text{Fe}_2\text{SiO}_4$ ,  $\text{MgSiO}_3$ ,  $\text{FeSiO}_3$ ,  $\text{Mg}_3\text{Al}_2\text{Si}_3\text{O}_{12}$ ,  $\text{Fe}_3\text{Al}_2\text{Si}_3\text{O}_{12}$ ,  $\text{CaSiO}_3$ , and  $\text{CaMgSi}_2\text{O}_6$ . We also present new reversal experimental data on the  $\alpha$ - $\beta$  transition in the system  $\text{Mg}_2\text{SiO}_4\text{-Fe}_2\text{SiO}_4$ , acquired using a newly developed multi-cell sample chamber technique in the multi-anvil apparatus. Finally, we review experimental results on mantle peridotite compositions and high-pressure phase transformations in systems related to the subducted oceanic lithosphere.

### HIGH-PRESSURE EXPERIMENTAL TECHNIQUES

There are three popularly used high-pressure devices for obtaining mantle phase equilibrium data, the piston-cylinder apparatus (up to 4 GPa), the multi-anvil apparatus (up to 27 GPa), and the diamond-anvil cell (up to at least 136 GPa, the core-mantle boundary pressure). Each apparatus has its own advantages and unique applications. The piston-cylinder apparatus (BOYD and ENGLAND 1960) provides accurate pressure measurements on a force-per-area basis especially using a low-friction NaCl cell assembly (MIRWALD *et al.*, 1975; MIRWALD and MASSONNE, 1980; BOHLEN and BOETTCHER, 1982). It has been extensively used for phase equilibrium measurements under crustal and upper mantle conditions (up to about 130 km in depth). For example, BOYD and ENGLAND (1964) determined the  $\text{Al}_2\text{O}_3$  content of orthopyroxene coexisting with garnet as a function of pressure and temperature. Subsequently, a number of experimental studies on solubility of  $\text{Al}_2\text{O}_3$  in orthopyroxene were carried

out in systems approaching peridotitic compositions (*e.g.*, BOYD, 1973; MACGREGOR, 1974; WOOD and BANNO, 1973; WOOD, 1974; HARLEY 1984; LEE and GANGULY 1988). The experimentally established geobarometers and geothermometers were crucial for constructing the history of mantle-derived garnet peridotites and played an important role in understanding the Earth's upper mantle. The success of applying geobarometers and geothermometers to mantle-derived rocks stimulated the field of experimental petrology. Piston-cylinder apparatus became standard equipment in experimental petrology laboratories.

The multi-anvil apparatus was designed to achieve pressures beyond the piston-cylinder range so that phase equilibrium measurements could be made under transition zone and lower mantle conditions (up to about 750 km in depth with tungsten carbide anvils). The laser-heated diamond-anvil cell technique is capable of achieving pressure-temperature conditions equivalent to that of the entire mantle, but it suffers from large temperature gradients, small sample size, and achieving equilibrium. In recent years, significant improvements in diamond cell laser-heating techniques have been made, especially in reducing the temperature gradient over a relatively large heating spot (30  $\mu\text{m}$ ) (SHEN *et al.*, 1996; MAO *et al.*, 1998). Potentially these improvements could revolutionize high-pressure experimental petrology. Our focus in this paper will be a discussion of the multi-anvil apparatus.

New experimental results on the olivine-wadsleyite ( $\alpha$ - $\beta$ ) transition in mantle compositions and phase relations in basaltic composition reported here were obtained using a multi-anvil apparatus at the Geophysical Laboratory. The apparatus consists of a retaining ring which houses six removable push wedges. The wedges transmit the uniaxial compressive force of the hydraulic ram onto the faces of a cube that is assembled from eight separate tungsten carbide cubes. Each of the eight tungsten carbide cubes has a truncated corner that rests against the face of an MgO octahedral pressure medium. The truncated cubes, which converge on the octahedron, are separated from one another by compressible pyrophyllite gaskets. Sample material is placed inside a furnace assembly that fits into a hole in the center of the octahedron (BERTKA and FEI, 1997). Two cell assemblies, 10/5 and 8/3 (octahedron edge length/truncated edge lengths), were used in this study. Rhenium foil (0.0025" thick) heaters with  $\text{LaCrO}_3$  insulator sleeves were used with the 8/3 assembly which is capable of generating a maximum pressure of 27 GPa and temperatures greater than 2500°C. Pressures at room temperature for both were calibrated using transitions in Bi at 2.55 GPa (I-II), and 7.7 GPa (III-V), in ZnS at 15.5 GPa (BLOCK, 1978), and in GaP at 23 GPa (DUNN and BUNDY, 1977). Temperature effect on the pressure calibration was evaluated by using phase transition boundaries in  $\text{SiO}_2$ ,  $\text{Fe}_2\text{SiO}_4$ ,  $\text{CaGeO}_3$ ,  $\text{MgSiO}_3$ , and  $\text{Mg}_2\text{SiO}_4$  as fixed high-temperature calibration points. Figure 1 shows the pressure calibration curves for the 8/3 assembly. Detailed pressure calibration at high temperatures showed significant temperature effect on the calibration (BERTKA and FEI, 1997; FROST and FEI, 1998; FEI and HIROSE, 1997). We found that the calibration curves at 1400°C and at 1000°C are the most and the least efficient ones, respectively. The effect of temperature on the pressure calibration can be qualitatively understood as the trade-off between material relaxation and thermal pressure at high temperature. The decrease in the efficiency of the pressure generation between room temperature and 1000°C is largely due to material relaxation. Between 1000°C and 1400°C, the thermal pressure becomes more important, resulting in

an increase in efficiency. The relaxation becomes a competing factor again at higher temperature ( $>1400^{\circ}\text{C}$ ) because of the decrease of material strength at very high temperature. The effect of relaxation and thermal pressure on pressure calibration as a function of temperature is illustrated in Fig. 2.

Sample temperature was measured with a W5%Re-W26%Re (Type C) thermocouple. Thermocouple placement in the sample chamber was axially for all the assemblies. The hot junction of the thermocouple is in direct contact with the sample container, even for our smallest assembly (8/3). Temperature gradients in cylindrical furnace assemblies commonly used with 10/5 and 8/3 octahedra are extensive,  $>100^{\circ}\text{C}/\text{mm}$  (GASPARIK, 1989). We reduced the sample temperature gradients by reducing the length of the sample container to about 0.5 mm for the 10/5 and 8/3 assemblies. Pyroxene thermometry experiments performed with the 8/3 assembly indicated that the temperature gradient across the sample length is  $<40^{\circ}\text{C}$  (BERTKA and FEI, 1997).

For the 10/5 assembly, we have developed a multi-cell sample chamber technique for high-precision experiments in the multi-anvil apparatus. Figure 3 shows the experimental configuration. The sample assembly consists of two 250- $\mu\text{m}$  thick metal (molybdenum or rhenium) disks separated by rhenium foils. At least seven 250- $\mu\text{m}$  diameter

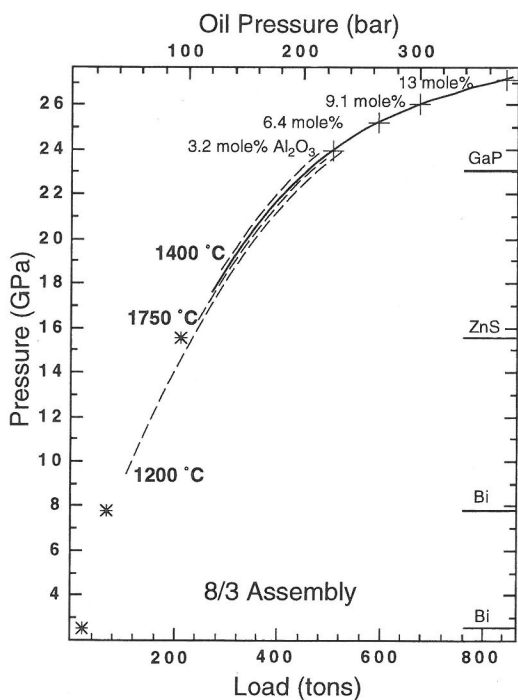


FIG. 1. Representative pressure calibration curves at 1200, 1400, and 1750 $^{\circ}\text{C}$  for a 1000-ton hydraulic press (dashed curves) (BERTKA and FEI, 1997; FROST and FEI, 1998) and at 1750 $^{\circ}\text{C}$  for a 1500-ton hydraulic press (solid curve) (HIROSE *et al.*, 1999). Selected maximum  $\text{Al}_2\text{O}_3$  solubilities (numbers in mole%) in orthorhombic perovskite were also plotted on the calibration curve (crosses). Stars indicate room-temperature calibration points for Bi, ZnS, and GaP.

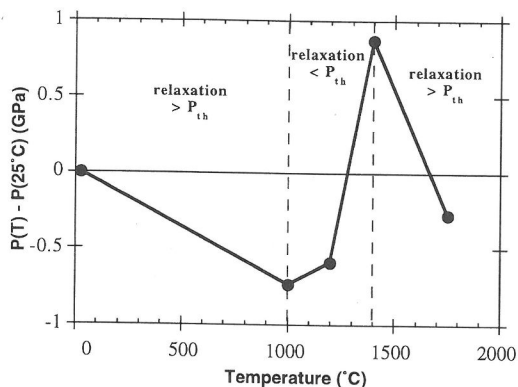


FIG. 2. Effect of relaxation and thermal pressure on pressure calibration as a function of temperature for an 8/3 assembly.

holes were drilled in each 1.5-mm diameter disk. Using this technique, starting materials with appropriate compositions loaded in the  $250 \times 250 \mu\text{m}$  sample cells were taken to identical high pressure and temperature conditions. In this manner compositional effect on phase transformations can be precisely determined. Reversal experiments can also be designed by loading two disks, one of which contains pre-synthesized high-pressure phase assemblages.

## HIGH-PRESSURE EXPERIMENTAL RESULTS ON MANTLE MINERALS

### $\text{SiO}_2$ Polymorphs and Phase Relations

The polymorphism of  $\text{SiO}_2$  at high pressure and temperature has been of great interest to petrologists and geophysicists because it can be used to indicate the deep origin of host minerals and rocks and to measure pressure generation in high-pressure apparatus. Quartz is a common crustal mineral and transforms to its high-pressure polymorph, coesite (COES, 1953), at high pressure ( $\sim 3$  GPa). Coesite further transforms to stishovite, a six-coordinated rutile form of silica, at higher pressure ( $\sim 9$  GPa) (STISHOV and POPOVA, 1961). In situ X-ray diffraction and Raman spectroscopic measurements (TSUCHIDA and YAGI, 1989; KINGMA *et al.*, 1995) revealed that stishovite transforms to a non-quenchable denser  $\text{CaCl}_2$ -type structure at about 50 GPa. Other possible post-stishovite phases at much higher pressures have also been proposed (*e.g.*, COHEN, 1992; TSE and KLUG, 1992; DUBROVINSKY *et al.*, 1997; TETER *et al.*, 1998).

The quartz-coesite and coesite-stishovite transitions have been frequently used as pressure calibration standards for high-pressure apparatus. The quartz-coesite transition is one of the most studied high-pressure transitions in piston-cylinder apparatus in which pressures were measured on a force-per-area basis (*e.g.*, BOYD, 1964; KITAHARA and

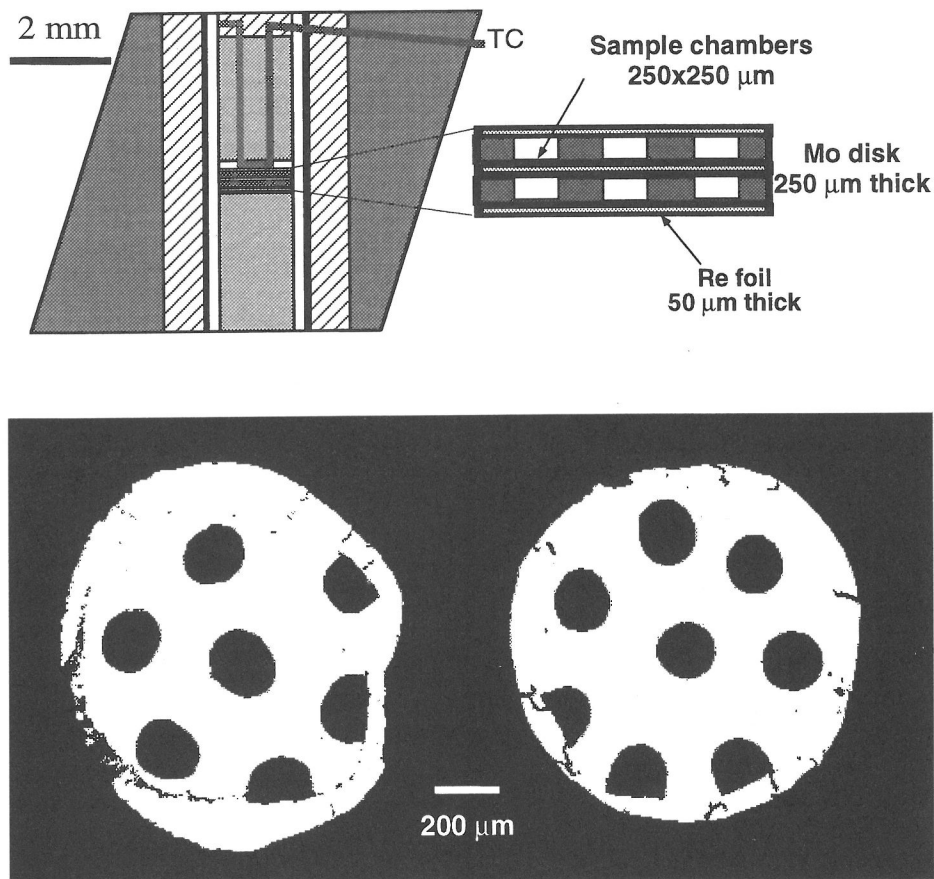


FIG. 3. Experimental configuration of a multi-cell technique in the multi-anvil apparatus. Sample chamber consists of two 250- $\mu\text{m}$  in thickness and 1.5-mm in diameter molybdenum disks separated by rhenium foils, loaded into a 10/5 assembly (BERTKA and FEI, 1997). The polished sections of the molybdenum disks (bottom) shows the 250- $\mu\text{m}$  diameter sample cells in which different starting materials were loaded to be subjected to the same pressure and temperature conditions.

KENNEDY, 1964; AKELLA, 1979; MIRWALD and MASSONNE, 1980; BOHLEN and BOETTCHER, 1982). Figure 4 shows the experimentally determined phase diagram of  $\text{SiO}_2$  at high pressure and temperature. The  $\alpha$ -quartz-coesite phase boundary was determined by BOHLEN and BOETTCHER (1982), with numerous tight reversals between 350°C and 1000°C. This boundary has been widely used for pressure calibration. Extrapolating the boundary to high temperature, it intersects with the  $\alpha$ - $\beta$  quartz transition boundary at 3.21 GPa and 1327°C. Using the quartz-coesite boundary determined by MIRWALD and MASSONNE (1980), the  $\alpha$ - $\beta$ -quartz-coesite triple point is located at 3.44 GPa and 1380°C. The discrepancy may arise from the correction for friction in the piston-cylinder apparatus.

High-pressure devices such as the multi-anvil apparatus and the diamond-anvil cell are capable of

generating much higher pressure than the piston-cylinder apparatus, but the pressures cannot be measured on a force-per-area basis. The coesite-stishovite transition boundary has been commonly used for pressure calibration at high temperature in the multi-anvil apparatus. Accurate determination of this boundary is crucial for establishing a pressure scale at high temperature. In situ X-ray diffraction measurements of this boundary at temperatures between 500°C and 1100°C were first carried out by YAGI and AKIMOTO (1976). Recent in situ measurements at temperatures between 950°C and 1530°C (ZHANG *et al.*, 1996) indicated that the  $dP/dT$  slope of the transition is much larger than that of YAGI and AKIMOTO (1976). New calorimetric data on coesite and stishovite and thermodynamic calculations (AKAOGI *et al.*, 1995; LIU *et al.*, 1996) support the new phase equilibrium data (Fig. 4).

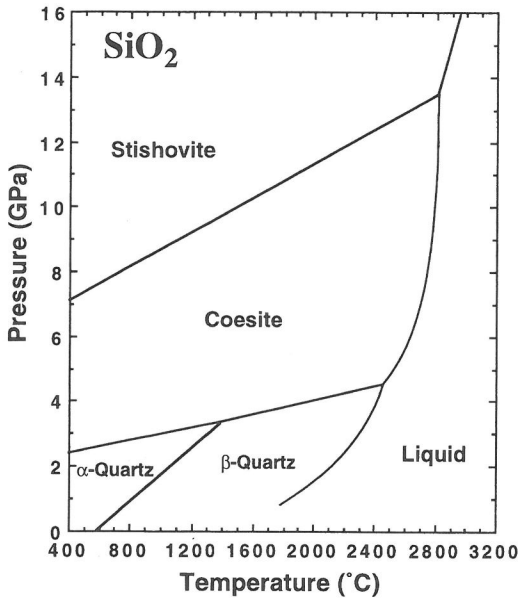


FIG. 4. Phase diagram of  $\text{SiO}_2$  at high pressure and temperature. Data sources for solid phase transitions are MIRWALD and MASSONNE (1980), BOHLEN and BOETTCHER (1982), and ZHANG *et al.* (1996). Melting curves are from JACKSON (1976), KANZAKI (1990), and ZHANG *et al.* (1993).

Coesite (or retrograde quartz) has been found in ultra high-pressure metamorphic rocks (*e.g.*, LIU and ZHANG, 1996; ZHANG *et al.*, 1996) and as mineral inclusion in eclogitic diamonds (*e.g.*, GURNEY, 1989; MEYER, 1987; MEYER *et al.*, 1995; SOBOLEV *et al.*, 1995, 1998). The occurrences of coesite in metamorphic rocks indicate that the host rocks were subjected to pressures equivalent to depths of at least 80–100 km. Stishovite has never been found in metamorphic or igneous rocks except in shocked rocks and meteorites. Its formation requires the origin of host rock to be deeper than 300 km, implying that no silica-saturated mantle rocks have been brought to the surface from a depth greater than 300 km.

#### $\text{Mg}_2\text{SiO}_4$ Polymorphs and Phase Relations

Olivine is one of the major constituents of mantle-derived rocks. Its high-pressure polymorphism has been extensively studied because of its connection to the 410-km and 660-km seismic velocity discontinuities. The phase relations for the three  $\text{Mg}_2\text{SiO}_4$  polymorphs (olivine,  $\beta$ -phase or wadsleyite, and spinel or ringwoodite) have been experimentally investigated by RINGWOOD and MAJOR (1970), SUIO (1972, 1977), KAWADA (1977), OHTANI (1979), FUKIZAWA (1982), SAWAMOTO (1986), KATSURA and ITO (1989), and MORISHIMA *et al.* (1994). Discrepancies in the loca-

tion of the phase boundaries by different investigators, especially in earlier studies, were largely due to different pressure scale at high temperatures. Recently in situ X-ray diffraction measurements of the olivine-wadsleyite ( $\alpha$ - $\beta$ ) transition boundary (MORISHIMA *et al.*, 1994) showed that the transition pressure is consistent with that of KATSURA and ITO (1989) at 1600°C, but it is about 0.5 GPa lower than that of KATSURA and ITO (1989) at 1100°C. Figure 5 shows the phase diagram of  $\text{Mg}_2\text{SiO}_4$  at high pressure and temperature based on the most recent experimental results.

The wadsleyite-spinel ( $\beta$ - $\gamma$ ) transition boundary determined by KATSURA and ITO (1989) has been widely used as a pressure calibration point at high temperature for multi-anvil apparatus. The exact location of this boundary is less certain because no in situ measurements have been made so far. However, existing experimental results by the quenching method (SUIO, 1977; SAWAMOTO, 1986; KATSURA and ITO, 1989) are generally consistent.

$\text{Mg}_2\text{SiO}_4$ -spinel decomposes into  $\text{MgSiO}_3$ -perovskite and MgO-periclase at lower mantle pressures. ITO and TAKAHASHI (1989) determined the spinel = perovskite + periclase transformation boundary by

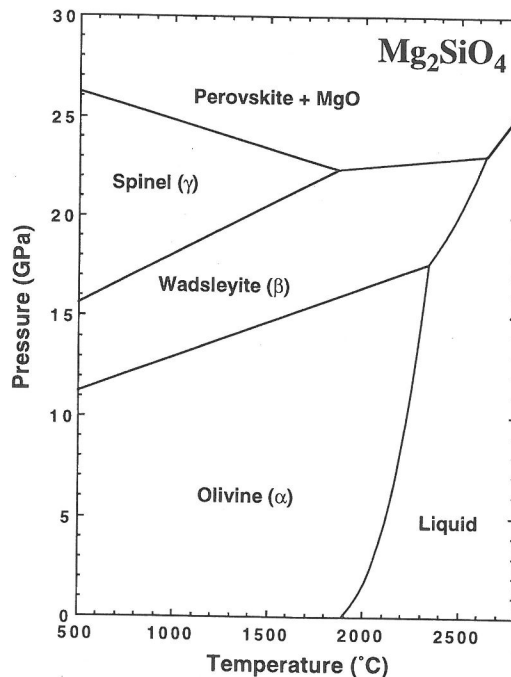


FIG. 5. Phase diagram of  $\text{Mg}_2\text{SiO}_4$  at high pressure and temperature. Data sources for solid phase transformations are KATSURA and ITO (1989) and ITO and TAKAHASHI (1989). Melting curves are from DAVIS and ENGLAND (1964) and PRESNALL and WALTER (1993).

the quenching technique. The pressure calibration for determining the boundary was based on a phase transition in GaP at 23 GPa and room temperature, and other phase transitions at lower pressures (< 21 GPa). Temperature effect on the pressure calibration was corrected on the basis of previously determined phase boundaries such as the  $\alpha$ - $\beta$  and  $\beta$ - $\gamma$  transitions. The consistency and accuracy of such pressure calibrations need to be further verified by in situ measurements. However, until reliable in situ measurements become available, the boundary reported by ITO and TAKAHASHI (1989) serves as a reference for inter-laboratory comparison of the high-temperature pressure scale between 22 GPa and 25 GPa.

#### $Fe_2SiO_4$ Polymorphs and Phase Relations

$Fe_2SiO_4$ , unlike  $Mg_2SiO_4$ , directly transforms from olivine ( $\alpha$ ) to spinel ( $\gamma$ ) at high pressure. The transition has been experimentally studied using the quench technique (AKIMOTO *et al.*, 1965, 1967) and in situ X-ray diffraction (INOUE, 1975; SUNG and BURNS, 1976; FURNISH and BASSETT, 1983; YAGI *et al.*, 1987). YAGI *et al.* (1987) accurately determined the equilibrium phase boundary between 1073 and 1473 K using synchrotron X radiation. The transition pressures are defined by  $P(\text{GPa}) = 2.75 + 0.0025T(^{\circ}\text{C})$ .  $\gamma$ - $Fe_2SiO_4$  dissociates to  $Fe_xO$  (wüstite) and  $SiO_2$  (stishovite) at higher pressure. KATSURA *et al.* (1998) showed that the post-spinel transition in  $Fe_2SiO_4$  occurs at 17.3 GPa with no apparent temperature dependence. Figure 6 shows the phase diagram of  $Fe_2SiO_4$  at high pressure and temperature.

#### Phase Relations in the System $Mg_2SiO_4$ - $Fe_2SiO_4$

The olivine-wadsleyite-spinel ( $\alpha$ - $\beta$ - $\gamma$ ) transitions in the  $Mg_2SiO_4$ - $Fe_2SiO_4$  system have been investigated by KATSURA and ITO (1989) in the Mg-rich region and by AKIMOTO (1987) in the Fe-rich region. Because wadsleyite in  $Fe_2SiO_4$  is not stable, the  $(Mg,Fe)_2SiO_4$  wadsleyite solid solution does not extend into the Fe-rich region. The maximum FeO solubility in the wadsleyite structure is about 28 mole% at 1600°C (KATSURA and ITO, 1989). Therefore, the transition sequence is from olivine to wadsleyite and to spinel in the Mg-rich region with increasing pressure, whereas the sequence is from olivine directly to spinel in the Fe-rich region. The  $\alpha$ - $\beta$  transition in the Mg-rich region has been studied in detail at 1200°C and 1600°C (KATSURA and ITO, 1989) because this transition may be responsible for the observed 410-km seismic velocity discontinuity in the Earth's mantle. Precise determination of the  $\alpha$ - $\beta$  transition boundaries is difficult because  $\alpha$  and  $\beta$

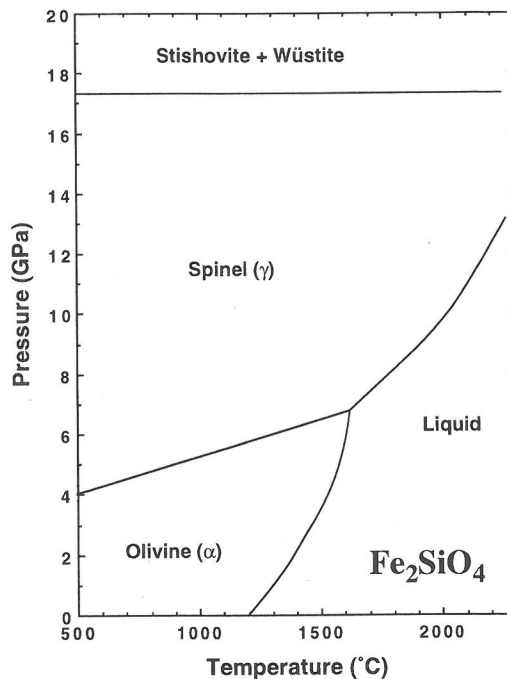


FIG. 6. Phase diagram of  $Fe_2SiO_4$  at high pressure and temperature. Data sources for solid phase transformations are YAGI *et al.* (1987) and KATSURA *et al.* (1998). Melting curves are from AKIMOTO *et al.* (1967) and OHTANI (1979).

phases coexist within a 2 GPa pressure interval, whereas the uncertainty in pressure determination in the multi-anvil experiments is about  $\pm 0.5$  GPa. Using the multi-cell sample chamber technique discussed above, we are able to determine the  $\alpha$ + $\beta$  two-phase loop precisely.

We conducted multi-anvil experiments in the  $Mg_2SiO_4$ - $Fe_2SiO_4$  system at 1400°C. Run duration for all experiments was 20 hours. In order to determine the  $\alpha$ - $\beta$  transition boundaries precisely, we needed to (1) determine the compositions of the coexisting  $\alpha$  and  $\beta$  phases at given pressure and temperature accurately, (2) establish a reliable and reproducible pressure calibration scale, and (3) obtain reversal points. Figure 7 shows the experimental results at 13.45 GPa and 1400°C. We loaded eight  $(Mg,Fe)_2SiO_4$  olivine starting materials, with compositions ranging from  $(Mg_{0.92}Fe_{0.08})_2SiO_4$  to  $(Mg_{0.78}Fe_{0.22})_2SiO_4$  (at 2 mole %  $Fe_2SiO_4$  intervals), into separate sample cells in a single run. Upon quenching from 13.45 GPa and 1400°C, the starting materials with compositions from  $(Mg_{0.92}Fe_{0.08})_2SiO_4$  to  $(Mg_{0.90}Fe_{0.10})_2SiO_4$  remained as a single  $\alpha$  phase, whereas the starting materials with compositions from  $(Mg_{0.80}Fe_{0.20})_2SiO_4$  to  $(Mg_{0.78}Fe_{0.22})_2SiO_4$  transformed into the high-pressure  $\beta$  phase. Two coexisting  $\alpha$  and  $\beta$  phases were observed in compositions between

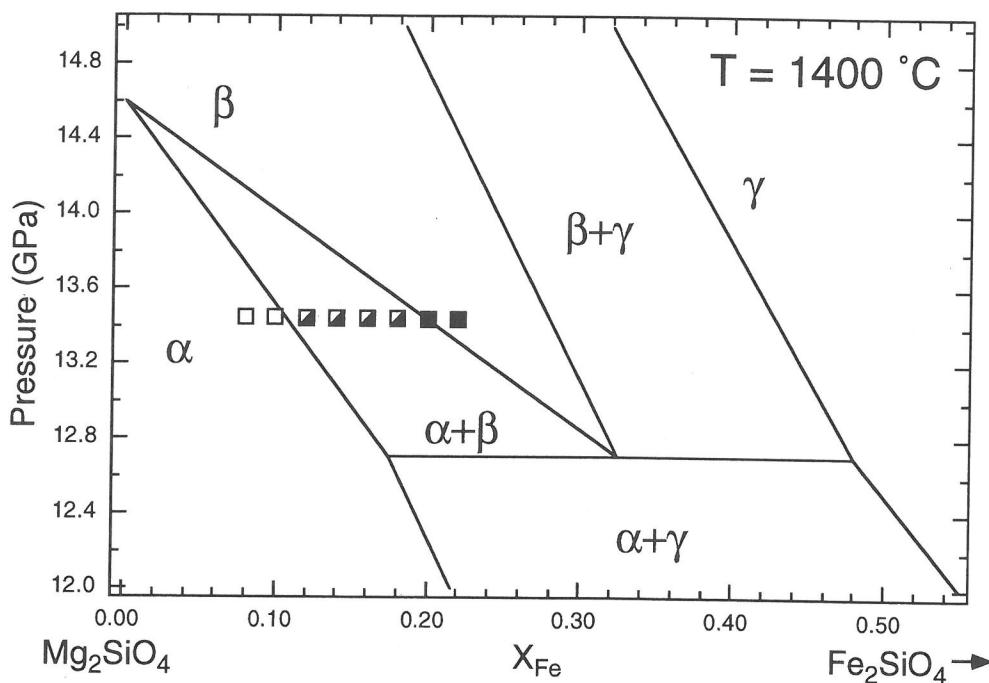


FIG. 7. The olivine-wadsleyite ( $\alpha$ - $\beta$ ) transition in the system  $\text{Mg}_2\text{SiO}_4$ - $\text{Fe}_2\text{SiO}_4$  at 13.45 GPa and 1400°C. Eight olivine samples with different compositions were loaded into separate sample cells in a single run. Single  $\alpha$  phase was observed for Fo92 and Fo90 (open squares), whereas single  $\beta$  phase was observed for Fo80 and Fo78 (solid squares). The half-filled symbols show the field where the  $\alpha$  and  $\beta$  phases coexist.

$(\text{Mg}_{0.90}\text{Fe}_{0.10})_2\text{SiO}_4$  and  $(\text{Mg}_{0.80}\text{Fe}_{0.20})_2\text{SiO}_4$ . Therefore, the transition boundary between single  $\alpha$  phase and the  $\alpha+\beta$  two-phase region was defined by a composition between  $(\text{Mg}_{0.90}\text{Fe}_{0.10})_2\text{SiO}_4$  and  $(\text{Mg}_{0.88}\text{Fe}_{0.12})_2\text{SiO}_4$ , whereas the boundary between single  $\beta$  phase and the  $\alpha+\beta$  two-phase region was defined by a composition between  $(\text{Mg}_{0.82}\text{Fe}_{0.18})_2\text{SiO}_4$  and  $(\text{Mg}_{0.80}\text{Fe}_{0.20})_2\text{SiO}_4$ . Phase modal abundances indicate that the  $\alpha$ - $\alpha+\beta$  boundary is closer to  $(\text{Mg}_{0.90}\text{Fe}_{0.10})_2\text{SiO}_4$  composition than  $(\text{Mg}_{0.88}\text{Fe}_{0.12})_2\text{SiO}_4$  composition, and the  $\alpha+\beta$ - $\beta$  boundary is closer to  $(\text{Mg}_{0.80}\text{Fe}_{0.20})_2\text{SiO}_4$  composition than  $(\text{Mg}_{0.82}\text{Fe}_{0.18})_2\text{SiO}_4$  composition. Microprobe analyses of the four samples with coexisting  $\alpha$  and  $\beta$  phases showed that the average compositions (Fe/[Fe+Mg] ratios) of the coexisting  $\alpha$  and  $\beta$  phases were  $0.106\pm 0.005$  and  $0.193\pm 0.006$ , respectively. Using this method, we have determined compositions of the coexisting  $\alpha$  and  $\beta$  phases at three different pressures, as listed in Table 1 and shown in Fig. 8.

Sample pressures in the multi-anvil experiments were determined from calibration curves established by calibrating oil pressure of the hydraulic press against fixed pressure calibration points. The precision of pressure determination relies on the reproducibility of the runs which is directly related to consistency of assembly preparation. Because the assembly

for the multi-cell sample chamber is made to be identical as possible, the reproducibility of pressure for this assembly should be very good. Our experi-

Table 1. Compositions of the coexisting  $\alpha$  and  $\beta$  phases at different pressures and 1400 °C.

P, GPa	$X_{\text{Fe}}^{\alpha}$	$X_{\text{Fe}}^{\beta}$
14.7	-	0.000
14.3	0.000	-
13.9	0.065(4)	0.120(4)
13.45	0.106(5)	0.193(6)
13.35	0.118(5)	0.212(3)
13.35*	0.111(4)	0.216(5)
13.0	0.149(5)	0.283(2)
12.9	0.160(2)	0.293(3)
12.9*	0.154(3)	0.289(3)

\*Reversal experiments. Values in parentheses represent the standard deviation in the last digits

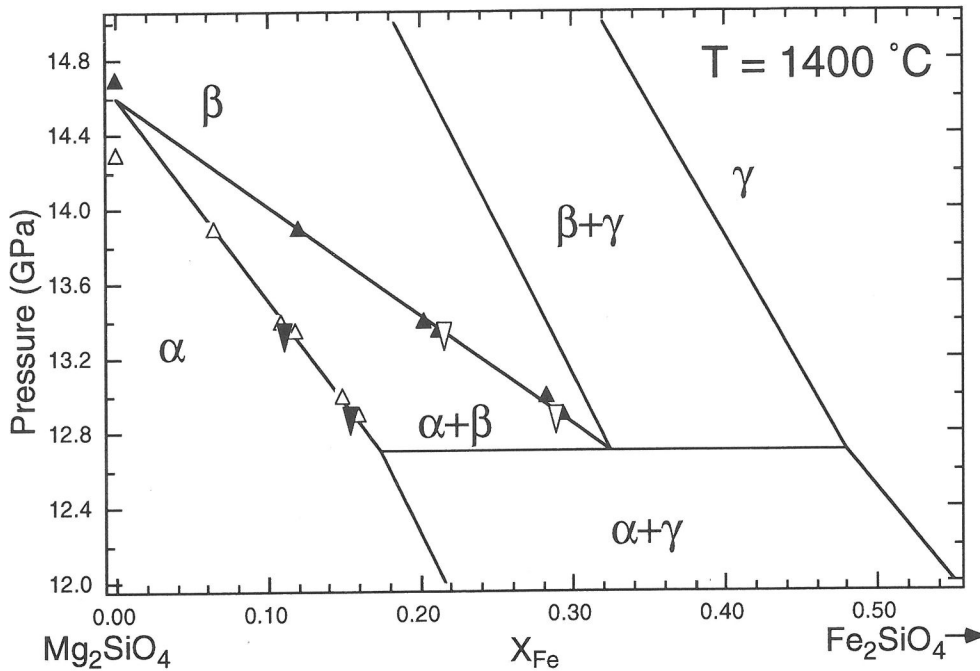


FIG. 8. Experimentally determined olivine-wadsleyite ( $\alpha$ - $\beta$ ) transition boundaries in the system  $\text{Mg}_2\text{SiO}_4$ - $\text{Fe}_2\text{SiO}_4$  at  $1400\text{ }^{\circ}\text{C}$ , with reversal points. The open and solid triangles represent the compositions of the coexisting  $\alpha$  and  $\beta$ , respectively, when olivine solid solutions were used as the starting materials, whereas the reversed open and solid triangles represent the compositions of the coexisting  $\beta$  and  $\alpha$ , respectively, when pre-synthesized wadsleyite solid solutions were used as the starting materials.

mental results confirmed the consistency in pressure calibration. Using an established calibration curve (Fig. 9), we determined the pressures for three ex-

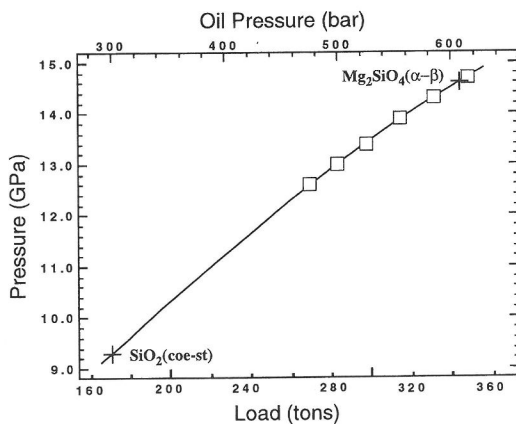


FIG. 9. Pressure calibration curve for the 10/5 assembly, used for determining the olivine-wadsleyite ( $\alpha$ - $\beta$ ) transition boundaries in the system  $\text{Mg}_2\text{SiO}_4$ - $\text{Fe}_2\text{SiO}_4$ . Crosses represent the coesite-stishovite transition in  $\text{SiO}_2$  and the  $\alpha$ - $\beta$  transition in  $\text{Mg}_2\text{SiO}_4$ . Open squares correlate to the pressures in Fig. 8.

periments at oil pressures of 500, 525, and 555 bars to be 13, 13.45, and 13.9 GPa, respectively. The compositions of  $\alpha$  and  $\beta$  phases for these three experiments vary linearly with pressure and the two lines intersect at 14.6 GPa and  $\text{Mg}_2\text{SiO}_4$  composition (Fig. 8). The intersected point marks the  $\alpha$ - $\beta$  transition in  $\text{Mg}_2\text{SiO}_4$ , which is consistent with the transition boundary determined by KATSURA and ITO (1989).

Reversal experiments were performed at 12.9 and 13.35 GPa, using pre-synthesized wadsleyite ( $\beta$ -phase) solid solutions as the starting materials. For the reversal experiment at 12.9 GPa, we first quenched a multi-cell sample disk from 14.2 GPa and  $1400\text{ }^{\circ}\text{C}$  and confirmed by Raman measurements that each of the  $(\text{Mg}_{0.90}\text{Fe}_{0.10})_2\text{SiO}_4$ ,  $(\text{Mg}_{0.88}\text{Fe}_{0.12})_2\text{SiO}_4$ , and  $(\text{Mg}_{0.84}\text{Fe}_{0.16})_2\text{SiO}_4$  starting materials transformed into  $\beta$ -phase. We then reloaded this sample disk together with another disk containing olivine starting materials into a new assembly for the reversal experiment at 12.9 GPa. The compositions ( $\text{Fe}/[\text{Fe}+\text{Mg}]$  ratios) of the coexisting  $\alpha$  phase are 0.118 and 0.111, respectively, using  $\alpha$  and  $\beta$  phases as the starting materials, whereas the compositions of the coexisting  $\beta$  phase are 0.212 and

0.216, respectively (Table 1 and Fig. 8). A similar procedure was used for the reversal experiment at 13.35 GPa and the results are shown in Table 1.

The wadsleyite-spinel ( $\beta$ - $\gamma$ ) transition boundaries in the  $\text{Mg}_2\text{SiO}_4$ - $\text{Fe}_2\text{SiO}_4$  system at 1200°C and 1600°C have been determined by KATSURA and ITO (1989). At higher pressures, spinel breaks down into silicate perovskite plus magnesiowüstite in the Mg-rich region and into magnesiowüstite plus stishovite in the Fe-rich region. The transformation from spinel to a perovskite assemblage is believed to be responsible for the 660-km seismic discontinuity and its boundaries have been determined in the Mg-rich region at 1100°C and 1600°C (ITO and TAKAHASHI, 1989). Recently AKAOGI *et al.* (1998) determined the postspinel transformation in the Fe-rich region at 1600°C. The phase diagram of postspinel transformations over an entire composition range in the  $\text{Mg}_2\text{SiO}_4$ - $\text{Fe}_2\text{SiO}_4$  system at 1600°C is shown in Fig. 10.

(Mg,Fe)SiO<sub>3</sub> perovskite forms limited solid solution which does not extend into the Fe-rich region. The maximum solubility of FeSiO<sub>3</sub> in the perovskite structure is defined by the reaction (Mg,Fe)SiO<sub>3</sub> (pv) = (Mg,Fe)O (mw) + SiO<sub>2</sub> (st). Recent experimental results showed that the maximum solubility of Fe-SiO<sub>3</sub> in the perovskite is a function of temperature and pressure (FEI *et al.*, 1996; MAO *et al.*, 1997). It

increases from 0.05 at 1000°C to 0.12 at 1750°C at 26 GPa, obtained by using the multi-anvil apparatus (FEI *et al.*, 1996). Laser-heated diamond cell experiments up to 55 GPa (MAO *et al.*, 1997) demonstrated that the maximum FeSiO<sub>3</sub> solubility increases rapidly with increasing pressure. About 28 mole % FeSiO<sub>3</sub> can be dissolved into the perovskite structure at 50 GPa and 1600°C.

#### *MgSiO<sub>3</sub> Polymorphs and Phase Relations*

There are at least six MgSiO<sub>3</sub> polymorphs (protoenstatite, orthoenstatite, clinoenstatite, non-cubic garnet, ilmenite and perovskite). Orthoenstatite transforms to a high-pressure clinoenstatite at about 8.1 GPa and 1000°C with a positive dP/dT slope of 0.0031 GPa/°C (PACALO and GASPARIK, 1990). With increasing pressure, the high-pressure clinoenstatite transforms into a two-phase (wadsleyite + stishovite or spinel + stishovite) region which separates the phase fields of pyroxene and ilmenite in polymorphic transitions. At temperatures higher than 1700°C, pyroxene directly transforms to a tetragonal garnet phase (majorite) at about 17 GPa (SAWAMOTO, 1987). The ilmenite-perovskite transition occurs at 24.3 GPa and 1000°C with a negative dP/dT slope of -0.0025 GPa/°C (ITO and TAKAHASHI, 1989). The transition boundary [P(GPa) = 26.8 - 0.0025T(°C)] has been commonly used as a pressure calibration standard at high temperature. The majorite-perovskite transition boundary has not been well determined because of its extremely high temperature conditions (>2000°C). Thermodynamic calculations showed that the boundary has a positive dP/dT slope (YUSA *et al.*, 1993). Recent experimental results on the majorite-perovskite transition in Al-bearing system also indicated a positive dP/dT slope of the transition (FEI and HIROSE, 1997). Figure 11 summarizes experimental results on phase relations in MgSiO<sub>3</sub> at high pressure and temperature.

#### *Phase Transformations in Mg<sub>3</sub>Al<sub>2</sub>Si<sub>3</sub>O<sub>12</sub>*

Pyrope (Mg<sub>3</sub>Al<sub>2</sub>Si<sub>3</sub>O<sub>12</sub>) transforms to ilmenite structure at about 24 GPa and 1000°C (KANZAKI, 1987). At higher temperatures, Mg<sub>3</sub>Al<sub>2</sub>Si<sub>3</sub>O<sub>12</sub>-ilmenite is not stable and pyrope breaks down into Al-bearing silicate perovskite plus corundum at about 26 GPa (IRIFUNE *et al.*, 1996; FEI and HIROSE, 1997). With increasing pressure, the Al<sub>2</sub>O<sub>3</sub> solubility in perovskite increases. Orthorhombic perovskite with pyrope composition ultimately forms at about 37 GPa (ITO *et al.*, 1998).

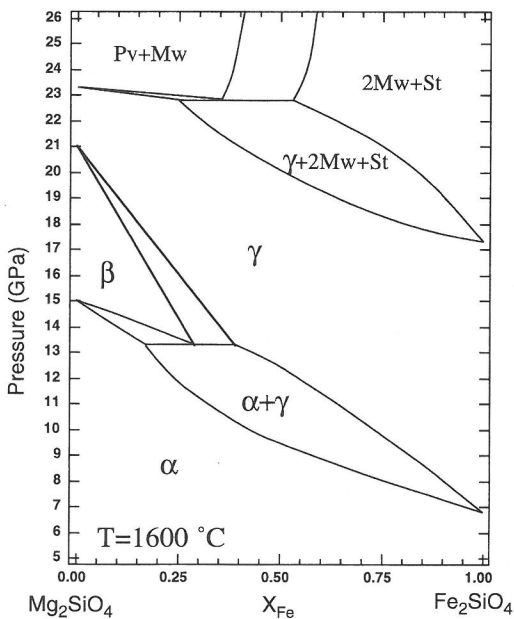


FIG. 10. Phase diagram in the system  $\text{Mg}_2\text{SiO}_4$ - $\text{Fe}_2\text{SiO}_4$  at 1600°C. Data sources are KATSURA and ITO (1989), ITO and TAKAHASHI (1989), FEI *et al.* (1991), and AKAOGI *et al.* (1998).

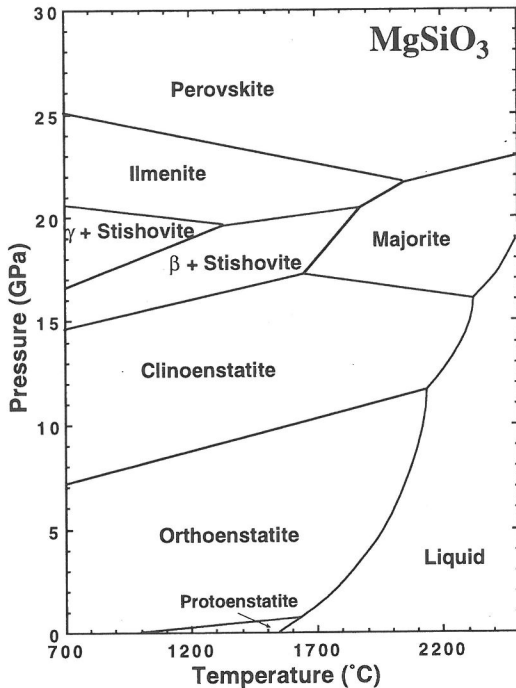


FIG. 11. Phase diagram of  $\text{MgSiO}_3$  at high pressure and temperature. Data sources for solid phase transformations are SAWAMOTO (1987), PACALO and GASPARIK (1990), and ITO and TAKAHASHI (1989). Melting curves are from BOYD *et al.* (1964) and PRESNALL and GASPARIK (1990).

#### Phase Relations in the System $\text{MgSiO}_3\text{-Mg}_3\text{Al}_2\text{Si}_3\text{O}_{12}$

Chemical analyses of mantle-derived garnet peridotites and high-pressure experimental results in the enstatite-pyrope system indicated that substantial amount of  $\text{Al}_2\text{O}_3$  could be dissolved into orthopyroxene coexisting with garnet (*e.g.*, BOYD, 1973). The  $\text{Al}_2\text{O}_3$  solubility in orthopyroxene is strongly dependent on pressure and temperature, which forms the basis for pyroxene geobarometers and geothermometers. Extensive experimental studies on the solubility of  $\text{Al}_2\text{O}_3$  in orthopyroxene were carried out at pressures between 2 GPa and 4 GPa in the piston-cylinder apparatus in order to establish an accurate geobarometer for constructing the history of mantle-derived garnet peridotites (*e.g.*, BOYD, 1973; MACGREGOR, 1974; WOOD and BANNO, 1973; WOOD, 1974; HARLEY, 1984; LEE and GANGULY, 1988). At higher pressures, the solubility of enstatite ( $\text{MgSiO}_3$ ) in pyrope ( $\text{Mg}_3\text{Al}_2\text{Si}_3\text{O}_{12}$ ) increases (AKAOGI and AKIMOTO, 1977; KANZAKI, 1987; AKAOGI *et al.*, 1987; GASPARIK, 1992) and the stability field of majorite solid solution expands with increasing temperature because of the formation of  $\text{MgSiO}_3$ -majorite at high

temperatures ( $> \sim 1650^\circ\text{C}$ ). Figure 12 shows the phase relations in the system  $\text{MgSiO}_3\text{-Mg}_3\text{Al}_2\text{Si}_3\text{O}_{12}$  at  $1500^\circ\text{C}$  and  $1900^\circ\text{C}$ .

The majorite-perovskite transformation in the system  $\text{MgSiO}_3\text{-Mg}_3\text{Al}_2\text{Si}_3\text{O}_{12}$  has been studied at temperatures between  $1000^\circ\text{C}$  and  $2000^\circ\text{C}$  (KANZAKI, 1987; IRIFUNE *et al.*, 1996; FEI and HIROSE, 1997). The phase relations between 16 GPa and 27 GPa change dramatically as a function of temperature because of complex phase relations in the  $\text{MgSiO}_3$  end-member. The  $(\text{Mg,Al})(\text{Al,Si})\text{O}_3$  ilmenite solid solution extends to  $\text{Mg}_3\text{Al}_2\text{Si}_3\text{O}_{12}$  composition at  $1000^\circ\text{C}$  (KANZAKI, 1987). Its stability shrinks rapidly with increasing temperature, whereas the stability field of the majorite solid solution expands, resulting in coexistence of majorite and Al-bearing perovskite. At about 26.5 GPa, pyrope transforms to Al-bearing perovskite and corundum. The solubility of  $\text{Al}_2\text{O}_3$  in the perovskite structure, defining the complete transformation of majorite to perovskite, significantly increases with pressure from 1.4 mole% at 23 GPa to 13 mole% at 27 GPa at a temperature of  $1750^\circ\text{C}$  (FEI and HIROSE, 1997). FEI and HIROSE (1997) also found that the solubility of  $\text{Al}_2\text{O}_3$  in perovskite coexisting

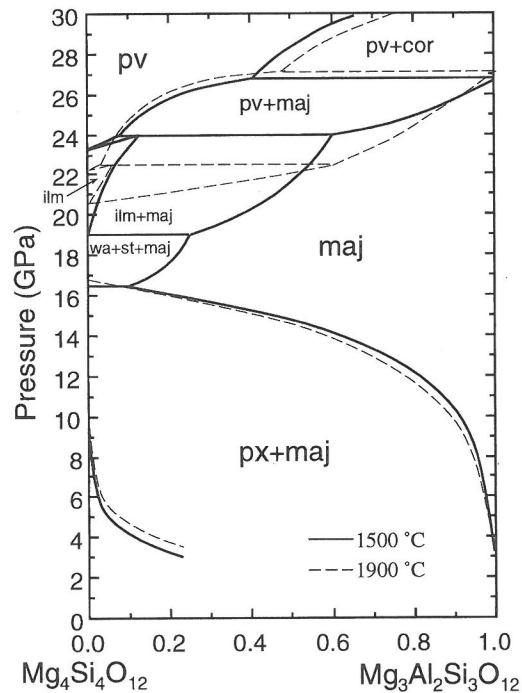


FIG. 12. Phase relations in the system  $\text{MgSiO}_3\text{-Mg}_3\text{Al}_2\text{Si}_3\text{O}_{12}$  at  $1500^\circ\text{C}$  (solid lines) and  $1900^\circ\text{C}$  (dashed lines). Data sources are AKAOGI *et al.* (1987), GASPARIK (1992), IRIFUNE *et al.* (1996), and FEI and HIROSE (1997). px, pyroxene; ilm, ilmenite; wa, wadsleyite; st, stishovite; pv, perovskite; cor, corundum; and maj, majorite.

with majorite decreases with increasing temperature, indicating that the majorite-perovskite transformation has a positive pressure-temperature slope. On the other hand, IRIFUNE *et al.* (1996) reported that the solubility of  $\text{Al}_2\text{O}_3$  in perovskite coexisting with corundum increasing with increasing temperature, implying the  $\text{Mg}_3\text{Al}_2\text{Si}_3\text{O}_{12}$ -perovskite formation boundary has a negative pressure-temperature slope. The combination of these two studies indicates that the perovskite-majorite-corundum univariant line shifts to higher pressure at higher temperature (Fig. 12).

*Phase Transformations in  $\text{FeSiO}_3$ ,  $\text{Fe}_3\text{Al}_2\text{Si}_3\text{O}_{12}$ ,  $\text{CaSiO}_3$ , and  $\text{CaMgSi}_2\text{O}_6$*

In the  $\text{FeSiO}_3$  system, perovskite, majorite and ilmenite are not stable. Ferrosillite ( $\text{FeSiO}_3$ ) transforms to spinel ( $\text{Fe}_2\text{SiO}_4$ ) plus stishovite ( $\text{SiO}_2$ ) at about 10 GPa (AKIMOTO and SYONO, 1970), and further dissociate to wüstite ( $\text{Fe}_x\text{O}$ ) plus stishovite at 17.3 GPa (KATSURA *et al.*, 1998). Phase relations in the system  $\text{MgSiO}_3$ - $\text{FeSiO}_3$  consist of the pyroxene-spinel-stishovite loop and the spinel-magnesiowüstite-stishovite loop in the Fe-rich region, whereas phase relations are very complex in the Mg-rich region because of complex phase relations in the  $\text{MgSiO}_3$  at high pressures and temperatures. There are limited experimental data that show the stability fields of  $(\text{Mg},\text{Fe})\text{SiO}_3$  ilmenite and majorite (ITO and YAMADA, 1982; KATO, 1986; OHTANI *et al.*, 1991). The calculated phase diagrams in the system  $\text{MgSiO}_3$ - $\text{FeSiO}_3$  best illustrate the changes of phase

relations at different temperatures (FABRICHNAYA, 1995).

Almandine ( $\text{Fe}_3\text{Al}_2\text{Si}_3\text{O}_{12}$ ) decomposes into a mixture of wüstite, corundum, and stishovite at high pressure (CONRAD, 1998; AKAOGI *et al.*, 1998). The dissociation occurs at about 21 GPa with a slightly negative  $dP/dT$  slope (AKAOGI *et al.*, 1998). The phase relations in the system  $\text{Mg}_3\text{Al}_2\text{Si}_3\text{O}_{12}$ - $\text{Fe}_3\text{Al}_2\text{Si}_3\text{O}_{12}$  have not been experimentally determined. However, interpretation from phase relations of the end-member indicates that the solubility of FeO in Al-bearing perovskite is limited, in addition to the change of  $\text{Al}_2\text{O}_3$  solubility in perovskite at pressures between 26 and 37 GPa.

Like the system  $\text{MgSiO}_3$ - $\text{Mg}_3\text{Al}_2\text{Si}_3\text{O}_{12}$ , the system  $\text{FeSiO}_3$ - $\text{Fe}_3\text{Al}_2\text{Si}_3\text{O}_{12}$  forms solid solutions by a heterovalent substitution FeSi-AlAl. The solubility of  $\text{FeSiO}_3$  in almandine ( $\text{Fe}_3\text{Al}_2\text{Si}_3\text{O}_{12}$ ) increases with increasing pressure (AKAOGI and AKIMOTO, 1977). The maximum solubility of  $\text{FeSiO}_3$  in almandine is about 40 mole% at 9 GPa and 1000°C. The effect of temperature on the phase relations has not been studied.

Clinopyroxene, garnet,  $(\text{Ca}, \text{Mg})\text{SiO}_3$  majorite, and  $\text{CaSiO}_3$  perovskite are the primary Ca-bearing phases in the Earth's mantle. In bulk mantle compositions,  $\text{CaSiO}_3$  perovskite first appears at pressures between 17 and 18 GPa (*e.g.*, CANIL, 1994), depending on the CaO content in the bulk compositions. In the  $\text{CaSiO}_3$  system,  $\text{CaSiO}_3$  walstromite transforms to  $\text{Ca}_2\text{SiO}_4 + \text{CaSi}_2\text{O}_5$  at about 10 GPa, and then to  $\text{CaSiO}_3$  perovskite at about 12 GPa. GASPARIK *et al.*

Table 2. Chemical compositions of bulk rocks

	Pyrolite R(1966)	Pyrolite S(1982)	Garnet Lherzolite PHN-1611	Spinel Lherzolite KLB-1	Piclogite DA(1989)	Herzburgite MB(1985)	MORB H(1998)
$\text{SiO}_2$	45.20	44.50	44.54	44.48	47.79	43.64	49.64
$\text{TiO}_2$	0.71	0.22	0.25	0.16	-	0.01	1.64
$\text{Al}_2\text{O}_3$	3.54	4.31	2.80	3.59	3.44	0.65	14.88
FeO	8.47	8.36	10.24	8.10	7.21	7.83	11.43
MnO	0.14	-	0.13	0.12	-	-	0.18
MgO	37.48	37.97	37.94	39.22	32.34	46.36	8.51
CaO	3.08	3.50	3.32	3.44	9.22	0.50	10.55
$\text{Na}_2\text{O}$	0.57	0.39	0.34	0.30	-	0.01	2.90
$\text{K}_2\text{O}$	0.13	-	0.14	0.02	-	-	0.12
$\text{Cr}_2\text{O}_3$	0.43	0.44	0.29	0.31	-	0.53	-
NiO	0.20	-	-	0.25	-	-	-

Data sources: R(1966), RINGWOOD (1966); S(1982), SUN (1982); PHN-1611, NIXON and BOYD (1973); KLB-1, TAKAHASHI (1986); DA(1989), DUFFY and ANDERSON (1989); MB(1985), MICHAEL and BONATTI (1985); H(1998), HIROSE *et al.* (1999).

(1994) determined the phase relations from 8 to 15 GPa. The phase boundaries between  $\text{CaSiO}_3$  walsstromite and  $\text{Ca}_2\text{SiO}_4 + \text{CaSi}_2\text{O}_5$  and between  $\text{Ca}_2\text{SiO}_4 + \text{CaSi}_2\text{O}_5$  and  $\text{CaSiO}_3$  perovskite are defined by  $P(\text{GPa}) = 7.9 + 0.0014T(^{\circ}\text{C})$  and  $P(\text{GPa}) = 9.0 + 0.0021T(^{\circ}\text{C})$ , respectively.

Diopside ( $\text{CaMgSi}_2\text{O}_6$ ) is an important Ca-bearing end-member of rock-forming pyroxenes. The breakdown reaction of diopside at high pressures has been experimentally studied by several investigators (IRIFUNE *et al.*, 1989; GASPARIK, 1990; CANIL, 1994). At pressures of 17–18 GPa, diopside decomposes to an assemblage of  $\text{CaSiO}_3$  perovskite and (Ca, Mg) $\text{SiO}_3$  majorite at temperatures greater than 1300°C or to an assemblage of  $\text{CaSiO}_3$  perovskite and  $\text{MgSiO}_3$  ilmenite at temperatures below 1300°C (CANIL, 1994). On the other hand, IRIFUNE *et al.* (1989) observed that diopside decomposes to an assemblage of  $\text{CaSiO}_3$  perovskite,  $\text{Mg}_2\text{SiO}_4$  spinel and  $\text{SiO}_2$  stishovite at 19 GPa and 1500°C. The discrepancy is related to uncertainty in determination of the  $\text{Mg}_2\text{SiO}_4$  spinel +  $\text{SiO}_2$  stishovite to  $\text{MgSiO}_3$  ilmenite transformation boundary because of kinetic problems and to uncertainty in pressure calibration. GASPARIK (1990) also studied the breakdown reaction of diopside in the enstatite-diopside join at high pressures and about 1650°C. The observed diopside breakdown products are  $\text{CaSiO}_3$  perovskite and (Ca, Mg) $\text{SiO}_3$  majorite at pressures above 17.5 GPa, consistent with the results of CANIL (1994). The coexisting (Ca, Mg) $\text{SiO}_3$  majorite, whose crystal chemistry was described by HAZEN *et al.* (1994), is rather enstatite-rich in composition (>75 mole % enstatite). However, at pressures between 15.7 and 17.5 GPa, GASPARIK (1990) reported a phase (designated as CM phase) that is compositionally diopside-rich (>80 mole % diopside). Further crystallographic study is required to address the nature of this phase.

#### HIGH-PRESSURE EXPERIMENTAL RESULTS ON BULK ROCKS

There are two competing petrological models of the mantle, pyrolite (or peridotite) and piclogite. Pyrolite, proposed by RINGWOOD (1962a), is an olivine-rich (~61% by volume) assemblage, whereas piclogite, proposed by BASS and ANDERSON (1984) and ANDERSON and BASS (1984), is a clinopyroxene-garnet rich, olivine-bearing rock. In the piclogite model, the olivine content is less than 50% by volume. By comparing seismic velocities in mantle minerals with seismic data, DUFFY and ANDERSON (1989) proposed a piclogite model consisting of 40% olivine, 37% clinopyroxene, 13% garnet, and 10% orthopyroxene.

Recent sound velocity and acoustic velocity measurements at high pressures indicate that an olivine amount of 38–50% in the upper mantle is required to satisfy the observed 410-km seismic discontinuity (LI *et al.*, 1998; ZHA *et al.*, 1997, 1998). The large uncertainty in olivine fraction of the mantle is largely due to the assumption of temperature effect on the velocity contrast across the discontinuity.

Pyrolite is a conceptual mixture comprised four parts of dunite and one part of basalt (RINGWOOD, 1962a). Its chemical composition has been revised through the years (*e.g.*, RINGWOOD, 1966, 1979; SUN, 1982). Table 2 lists two typical pyrolite compositions proposed by RINGWOOD (1966) and SUN (1982) that have been used as starting materials in high-pressure experiments. The composition is very similar to that of a sheared garnet lherzolite (PHN-1611) (NIXON and BOYD, 1973) and a spinel lherzolite (KLB-1)

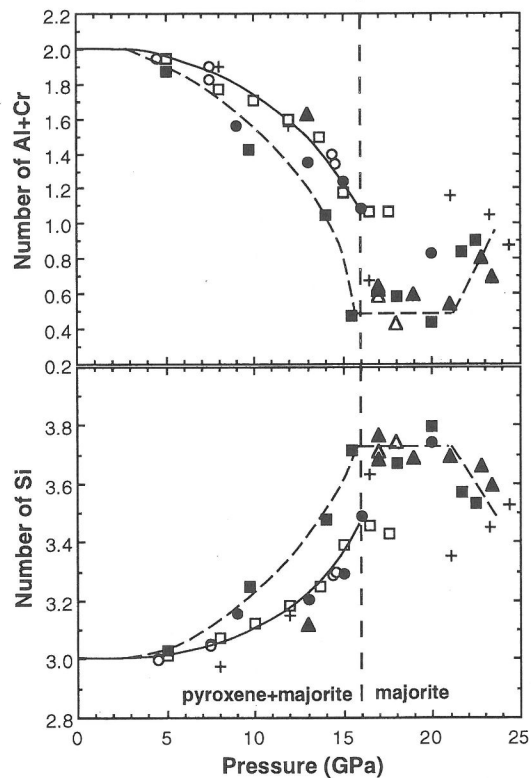


FIG. 13. Numbers of Al+Cr and Si atoms for 12 oxygens in the formula of majorite vs. pressure. Data sources: AKAOGI and AKIMOTO (1979) (open circles); HERZBERG and ZHANG (1996) (solid squares); CANIL (1991) (open triangles); IRIFUNE (1987) (open squares); TAKAHASHI and ITO (1987) (solid circles); IRIFUNE and RINGWOOD (1987); and BERTKA and FEI (1997). Data obtained at ~1200°C seem to follow the solid curve, whereas data at temperatures greater than 1600°C follow the dashed lines.

(TAKAHASHI, 1986) (Table 2), naturally occurring peridotites derived from the Earth's upper mantle. Both PHN-1611 and KLB-1 have been considered as candidates for undepleted mantle composition (SHIMIZU, 1974; TAKAHASHI, 1986) and widely used as starting materials for high-pressure experiments. In this section, we review high-pressure phase transformations in a garnet peridotite composition (PHN-1611) determined by AKAOGI and AKIMOTO (1979) and TAKAHASHI and ITO (1987) and in a pyrolite composition by IRIFUNE (1987) and IRIFUNE and ISHIKI (1998).

Harzburgite and mid-ocean ridge basalt (MORB) represent two important components of the oceanic lithosphere. Phase relations in those compositions at high pressures and temperatures are crucial for understanding the fate of subducted oceanic lithosphere and mantle dynamics. In this section we also review phase transformations in a harzburgite composition (IRIFUNE and RINGWOOD, 1987a) and in a MORB composition (IRIFUNE and RINGWOOD, 1987b, 1993; HIROSE *et al.*, 1999).

### Peridotite

Phase transformations in a garnet peridotite composition (PHN-1611) were determined up to lower mantle pressures (26 GPa) along a model geotherm (1500°–1600°C) (TAKAHASHI and ITO, 1987). The same composition was also studied up to 20.5 GPa in the temperature range 1050°–1200°C (AKAOGI and AKIMOTO, 1979). The major constituent minerals in PHN-1611 are olivine, orthopyroxene, Ca-rich clinopyroxene, and garnet. Orthopyroxene transforms to Ca-poor clinopyroxene at about 10 GPa. The solubility of pyroxene component in garnet increases significantly at pressures larger than 8 GPa, forming garnet solid solution (or majorite). Above 16 GPa, pyroxene dissolves into majorite completely. IRIFUNE (1987) investigated the pyroxene-garnet transformation in a 'pyrolite minus olivine' composition in great detail at pressures between 4 and 17.5 GPa. Figure 13 shows the changes of the numbers of Si and Al + Cr atoms in garnet (12 oxygen in the formula) as a function of pressure. Comparing data obtained from

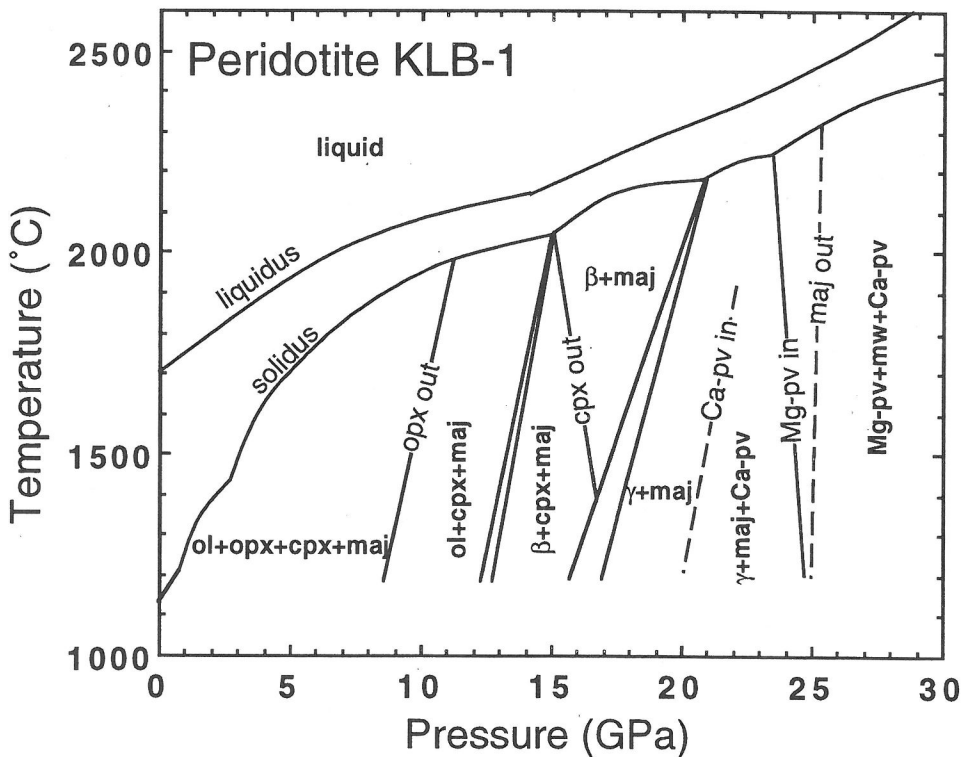


FIG. 14. Melting and sub-solid phase relations in peridotite KLB-1 at high pressures and temperatures. Data sources are TAKAHASHI (1986), TAKAHASHI and ITO (1987), ZHANG and HERZBERG (1994), and HERZBERG and ZHANG (1996).

different bulk composition over a large temperature range, a systematic temperature effect is shown at pressures below 16 GPa where clinopyroxene and majorite coexists. The data scattering in the majorite stability field is caused by the different  $\text{Al}_2\text{O}_3$  content in the systems and different coexisting phases at various pressures.

Pyrolite consists of about 60% olivine in volume. The  $\alpha$ - $\beta$  transition in olivine is considered to be responsible for the 410-km seismic discontinuity. This transition occurs at pressures between 13 and 16 GPa in a peridotite composition, depending on temperature. Recently, IRIFUNE and ISSHIKI (1998) narrowed the transition pressure to between 13 and 14 GPa at 1380°C in a pyrolite composition. They also demonstrated that the iron content in olivine changes as a function of pressure, effectively reducing the width of the two-phase loop. However, such a variation of iron content in olivine was not observed in experiments carried out at constant temperature (cf., AKAOGI and AKIMOTO, 1979; TAKAHASHI and ITO, 1987), except that the iron content in the  $\beta$ -phase above the transition pressure is slightly higher than that in the  $\alpha$ -phase below the transition boundary. The  $\beta$ - $\gamma$  transition in olivine was observed at pressures between 17 and 20 GPa at 1600°C in a garnet lherzolite composition (TAKAHASHI and ITO, 1987). There are very few experimental data points at pressures above 20 GPa.  $\text{CaSiO}_3$  perovskite, together with Mg-perovskite, magnesiowüstite, and majorite, was observed in an experiment at 24 GPa and 1600°C (TAKAHASHI and ITO, 1987). The formation of  $\text{CaSiO}_3$  perovskite in a natural peridotite KLB-1 is at pressures between 17 and 18 GPa (CANIL, 1994). All the  $\text{Al}_2\text{O}_3$  in the bulk rock should be ultimately incorporated into the orthorhombic perovskite structure at high pressure. However, it is not clear that an Al-rich phase would form in a peridotite composition at pressures near the spinel to perovskite plus magnesiowüstite transformation boundary, as reported by TAKAHASHI and ITO (1987).

Melting relations in peridotite KLB-1 have been reported up to 23 GPa (TAKAHASHI, 1986; ZHANG and HERZBERG, 1994; HERZBERG and ZHANG, 1996). Figure 14 summarizes melting and sub-solid phase relations at high pressures and temperatures. Mineral proportions in pyrolite as a function of pressure are shown in Fig. 15. ITA and STIXRUDE (1992) computed mineral proportion for a piclogite model as a function of depth. No high-pressure experiments have been conducted directly on a piclogite composition.

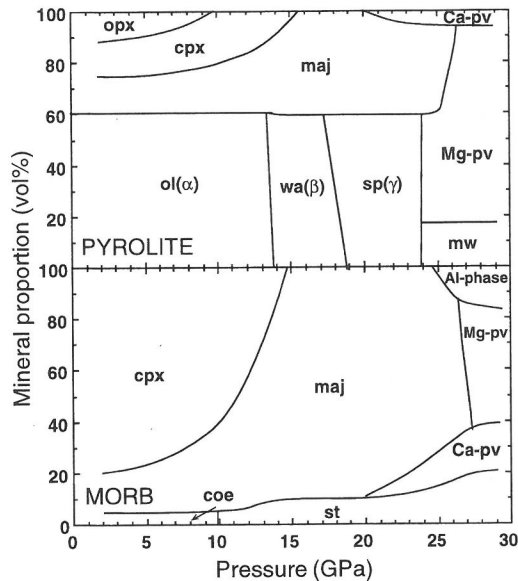


FIG. 15. Comparison of modal mineralogy (in volume %) between pyrolite and MORB as a function of pressure. Data sources are IRIFUNE and RINGWOOD (1987, 1993), IRIFUNE and ISSHIKI (1998), and HIROSE *et al.* (1999). ol, olivine; opx, orthopyroxene; cpx, clinopyroxene; maj, majorite; wa, wadsleyite; sp, spinel; mw, magnesiowüstite; Mg-pv, ferromagnesian silicate perovskite; Ca-pv,  $\text{CaSiO}_3$  perovskite; st, stishovite; and Al-phase, Al-rich phase with calcium ferrite structure.

#### Basalt and Harzburgite

The chemical composition of MORB is distinctly different from that of peridotites (Table 2). Because MORB has high Si, Al, Fe, and Na contents, its mineralogy at mantle pressures is very different from that of mantle peridotite (*e.g.*, IRIFUNE and RINGWOOD, 1987b, 1993; YASUDA *et al.*, 1994; HIROSE *et al.*, 1999). Garnet and clinopyroxene are the major constituent minerals in MORB at pressures below 10 GPa. With increasing pressure, clinopyroxene gradually dissolves into garnet, resulting in the formation of stishovite at pressures above 10 GPa.  $\text{CaSiO}_3$  perovskite starts to form at a pressure of 20 GPa, resulting from a decrease of the maximum solubility of CaO in majorite at high pressure. IRIFUNE and RINGWOOD (1993) reported an Al-rich phase with relatively high  $\text{Na}_2\text{O}$  content in MORB composition at pressures above 25 GPa. This phase was further confirmed in the study of HIROSE *et al.* (1999). It appears to have a calcium ferrite type structure, like the high-pressure polymorphs of  $\text{MgAl}_2\text{O}_4$  and  $\text{NaAlSiO}_4$  (IRIFUNE *et al.*, 1991; LIU, 1977). In addition, HIROSE *et al.* (1999) reported a new aluminocalcic phase (Al-Ca-phase) in MORB composition at

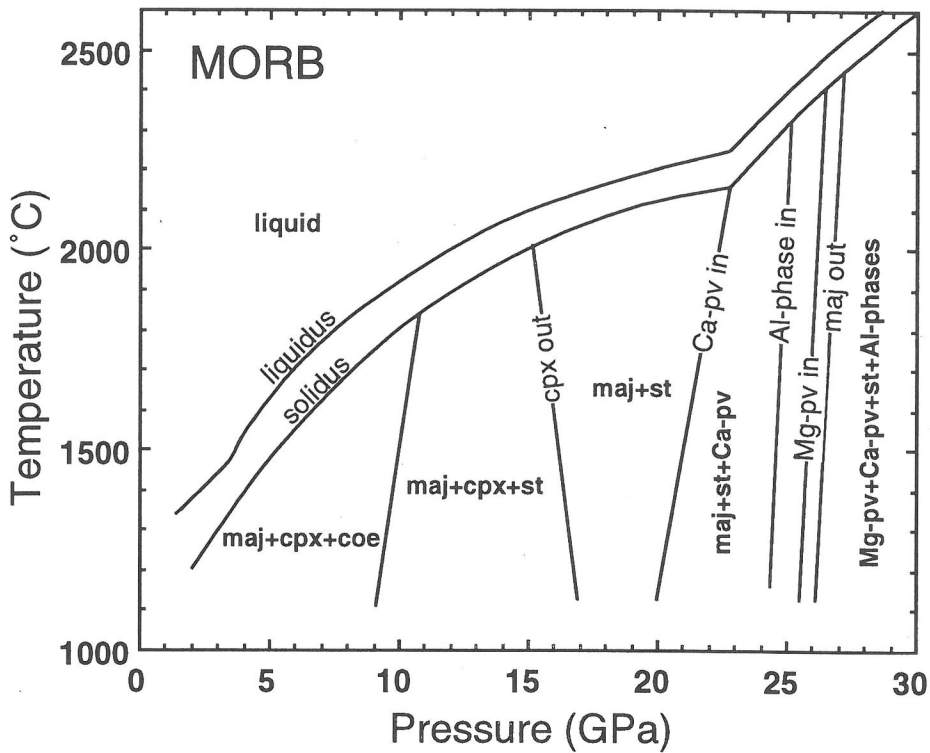


FIG. 16. Melting and sub-solid phase relations in MORB composition at high pressures and temperatures. Data sources are YASUDA *et al.* (1994), IRIFUNE and RINGWOOD (1993), and HIROSE *et al.* (1999).

26 GPa and near solidus temperature (2200°C). Further study is needed to determine the structure and stability field of this phase.

The majorite in MORB contains about 20 wt%  $\text{Al}_2\text{O}_3$  at 22 GPa, compared to about 8 wt%  $\text{Al}_2\text{O}_3$  in a peridotite composition. The higher  $\text{Al}_2\text{O}_3$  content of majorite in MORB results in a higher majorite-perovskite transition pressure in MORB relative to that in peridotite. HIROSE *et al.* (1999) reported that the majorite-perovskite transition starts at 26 GPa with small positive pressure-temperature slope (+0.0008  $\text{GPa}/^\circ\text{C}$ ) and completes within a 1 GPa interval. Figure 16 summarizes sub-solid phase and melting relations in MORB composition at high pressures and temperatures.

Harzburgite consists of about 82 wt% normative olivine and 18 wt% pyroxene-garnet component. It is compositionally distinct from that of the overlying basalt and that of the underlying residual lherzolite layer. Phase transformations in a harzburgite composition have been studied up to 26 GPa (IRIFUNE and RINGWOOD, 1987a). IRIFUNE and RINGWOOD (1987a) focused on the phase transformations in the pyroxene-garnet component. Because the  $\text{Al}_2\text{O}_3$  content in the system is relatively low (Table 2), the observed

phase transformations are similar to those in the  $\text{MgSiO}_3$ -rich region in the  $\text{MgSiO}_3$ - $\text{Mg}_3\text{Al}_2\text{Si}_3\text{O}_{12}$  system. Assemblages of majorite +  $\text{Mg}_2\text{SiO}_4$  spinel + stishovite and of majorite + ilmenite were observed at pressures between 19 and 22 GPa, and between 22 and 24 GPa, respectively. Like in the

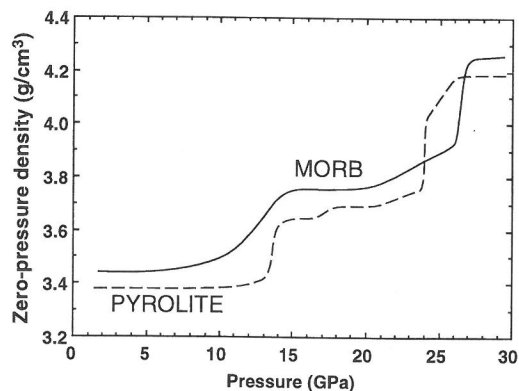


FIG. 17. Comparison of zero-pressure density changes in MORB (solid line) and pyrolite (dashed line) as a function of pressure. Data sources are IRIFUNE and RINGWOOD (1987, 1993), IRIFUNE and ISSHIKI (1998), and HIROSE *et al.* (1999).

simple system, the stability fields of  $\text{Mg}_2\text{SiO}_4$  spinel + stishovite and ilmenite are dependent on temperature.

Phase transformations in pyrolite and MORB control mantle density variations as a function of depth and play an important role in mantle dynamics. Former basaltic crust in a subducted slab has a higher density than the surrounding pyroclitic mantle above the 660-km discontinuity marked by perovskite formation in pyrolite (Fig. 17). It is less dense than the surrounding mantle just below the 660-km discontinuity. Once it transforms to perovskite lithology at about 720-km depth, its density significantly increases and it becomes denser than the surrounding pyroclitic mantle (HIROSE *et al.*, 1999). The transformation to perovskite lithology in basalt at 720 km depth could drive slab penetration into the deep mantle.

*Acknowledgments*—We wish to thank M. Akaogi and E. Takahashi for reviews of the paper. This work was supported by grant EAR-9418945 of the National Science Foundation and by the Carnegie Institution of Washington.

## REFERENCES

- AKAOGI M. and AKIMOTO S. (1977) Pyroxene-garnet solid solution equilibria in the system  $\text{Mg}_4\text{Si}_4\text{O}_{12}$ - $\text{Mg}_3\text{Al}_2\text{Si}_3\text{O}_{12}$  and  $\text{Fe}_4\text{Si}_4\text{O}_{12}$ - $\text{Fe}_3\text{Al}_2\text{Si}_3\text{O}_{12}$  at high pressures and temperatures. *Phys. Earth Planet. Inter.* **15**, 90–106.
- AKAOGI M. and AKIMOTO S. (1979) High-pressure phase equilibria in a garnet hercynite, with special reference to  $\text{Mg}^{2+}$ - $\text{Fe}^{2+}$  partitioning among constituent minerals. *Phys. Earth Planet. Inter.* **19**, 31–51.
- AKAOGI M., NAVROTSKY A., YAGI T., and AKIMOTO S. (1987) Pyroxene-garnet transition: Thermochemistry and elasticity of garnet solid solutions, and application to a pyrolite mantle. In *High Pressure Research in Mineral Physics* (eds. M. H. MANGHNANI and Y. SYONO), pp. 251–260, American Geophysical Union, Washington, DC.
- AKAOGI M., YUSA H., SHIRAIISHI K., and SUZUKI T. (1995) Thermodynamic properties of  $\alpha$ -quartz, coesite, and stishovite and equilibrium phase relations in high pressures and high temperatures. *J. Geophys. Res.* **100**, 22337–22347.
- AKAOGI M., OHMURA N., and SUZUKI T. (1998) High-pressure dissociation of  $\text{Fe}_3\text{Al}_2\text{Si}_3\text{O}_{12}$  garnet: phase boundary determined by phase equilibrium experiments and calorimetry. *Phys. Earth Planet. Inter.* **106**, 103–113.
- AKAOGI M., KOJITANI H., MATSUZAKA K., SUZUKI T., and ITO E. (1998) Postspinel transformations in the system  $\text{Mg}_2\text{SiO}_4$ - $\text{Fe}_2\text{SiO}_4$ : Element partitioning, calorimetry, and thermodynamic calculation. In *Properties of Earth and Planetary Materials at High Pressure and Temperature* (eds. M. H. MANGHNANI and T. YAGI) pp. 373–384, American Geophysical Union, Washington, DC.
- AKELLA J. (1979) Quartz = coesite transition and the comparative friction measurements in piston-cylinder apparatus using talc-alsimag-glass (TAG) and NaCl high-pressure cells. *Neues Jahrb. Mineral. Monatsh.* **5**, 217–224.
- AKIMOTO S. (1987) High-pressure research in geophysics: past, present and future. In *High Pressure Research in Mineral Physics* (eds. M. H. MANGHNANI and Y. SYONO), pp. 1–13, Terra Publications, Tokyo.
- AKIMOTO S. and IDA Y. (1966) High pressure synthesis of  $\text{Mg}_2\text{SiO}_4$  spinel. *Earth Planet. Sci. Lett.* **1**, 358–359.
- AKIMOTO S. and SYONO Y. (1970) High-pressure decomposition of the system  $\text{FeSiO}_3$ - $\text{MgSiO}_3$ . *Phys. Earth Planet. Inter.* **3**, 186–188.
- AKIMOTO S., FUJISAWA H., and KATSURA T. (1965) Olivine-spinel transition in  $\text{Fe}_2\text{SiO}_4$  and  $\text{Ni}_2\text{SiO}_4$ . *J. Geophys. Res.* **66**, 1969–1977.
- AKIMOTO S., KOMADA E., and KUSHIRO I. (1967) Effect of pressure on the melting of olivine and spinel polymorphs of  $\text{Fe}_2\text{SiO}_4$ . *J. Geophys. Res.* **68**, 679–686.
- ANDERSON D. L. and BASS J. D. (1984) Mineralogy and composition of the upper mantle. *Geophys. Res. Lett.* **11**, 637–640.
- BASS J. D. and ANDERSON D. L. (1984) Composition of the upper mantle: Geophysical tests of two petrological models. *Geophys. Res. Lett.* **11**, 237–240.
- BERNAL J. D. (1936) Discussion. *Observatory* **59**, 268.
- BERTKA C. M. and FEI Y. (1997) Mineralogy of Martian interior up to core-mantle boundary pressures. *J. Geophys. Res.* **102**, 5251–5264.
- BIRCH F. (1952) Elasticity and constitution of the Earth's interior. *J. Geophys. Res.* **57**, 227–286.
- BLOCK S. (1978) Round-robin study of the phase transformation in  $\text{ZnS}$ . *Acta. Cryst.* **A34**, Suppl. 316.
- BOHLEN S. R. and BOETTCHER A. L. (1982) The quartz = coesite transformation: A precise determination and the effects of other components. *J. Geophys. Res.* **87**, 7073–7078.
- BOYD F. R. (1964) Geological aspects of high-pressure research. *Science* **145**, 13–20.
- BOYD F. R. (1973) A pyroxene geotherm. *Geochim. Cosmochim. Acta* **37**, 2533–2546.
- BOYD F. R. and ENGLAND J. L. (1960) Apparatus for phase-equilibrium measurements at pressures up to 50 kilobars and temperatures up to 1750°C. *J. Geophys. Res.* **65**, 741–748.
- BOYD F. R. and ENGLAND J. L. (1964) The system enstatite-pyroxene. *Carnegie Inst. Washington Yearb.* **63**, 157–161.
- BOYD F. R., ENGLAND J. L., and DAVIS B. T. C. (1964) Effect of pressure on the melting and polymorphism of enstatite,  $\text{MgSiO}_3$ . *J. Geophys. Res.* **69**, 2101–2109.
- CANIL D. (1991) Experimental evidence for the exsolution of cratonic peridotite from high-temperature harzburgite. *Earth Planet. Sci. Lett.* **106**, 64–72.
- CANIL D. (1994) Stability of clinopyroxene at pressure-temperature conditions of the transition region. *Phys. Earth Planet. Inter.* **86**, 25–34.
- COES L. (1953) A new dense crystalline silica. *Science* **118**, 131–132.
- COHEN R. E. (1992) First-principles predictions of elasticity and phase transitions in high pressure  $\text{SiO}_2$  and geophysical implications. In *High Pressure Research: Application to Earth and Planetary Sciences* (eds. Y. SYONO and M. H. MANGHNANI) pp. 425–431, American Geophysical Union, Washington, DC.
- CONRAD P. G. (1998) The stability of almandine at high pressures and temperatures. In *Properties of Earth and Planetary Materials at High Pressure and Temperature* (eds. M. H. MANGHNANI and T. YAGI) pp. 393–399, American Geophysical Union, Washington, DC.

- DAVIS B. T. C. and ENGLAND J. L. (1964) The melting of forsterite up to 50 kbar. *J. Geophys. Res.* **69**, 1113–1116.
- DUBROVINSKY L. S., SAXENA S. K., LAZOR P., AHUJA R., ERIKSSON O., WILLS J. M. and JOHANSSON B. (1997) Experimental and theoretical identification of a new high pressure phase of silica. *Nature* **388**, 362–365.
- DUFFY T. S. and ANDERSON D. L. (1989) Seismic velocities in mantle minerals and the mineralogy of the upper mantle. *J. Geophys. Res.* **94**, 1895–1912.
- DUNN K. J. and BUNDY F. P. (1977) Materials and techniques for pressure calibration by resistance-jump transitions up to 500 kilobars. *Rev. Sci. Instrum.* **49**, 365–370.
- FABRICHNAYA O. B. (1995) Thermodynamic data for phases in the FeO-MgO-SiO<sub>2</sub> system and phase relations in the mantle transition zone. *Phys. Chem. Minerals* **22**, 323–332.
- FEI Y. and BERTKA C. M. (1996) The  $\alpha$ - $\beta$  transition in systems relevant to the upper mantle. *Eos* **77**, 649.
- FEI Y. and HIROSE K. (1997) Majorite-perovskite transformation in the system MgSiO<sub>3</sub>-Mg<sub>3</sub>Al<sub>2</sub>Si<sub>3</sub>O<sub>12</sub> at high P-T (abstract). *Eos* **78**, 761.
- FEI Y., MAO H. K., and MYSEN B. O. (1991) Experimental determination of element partitioning and calculation of phase relations in the MgO-FeO-SiO<sub>2</sub> system at high pressure and high temperature. *J. Geophys. Res.* **96**, 2157–2169.
- FEI Y., WANG Y., and FINGER L. W. (1996) Maximum solubility of FeO in (Mg,Fe)SiO<sub>3</sub>-perovskite as a function of temperature at 26 GPa: Implication for FeO content in the lower mantle. *J. Geophys. Res.* **101**, 11525–11530.
- FROST D. J. and FEI Y. (1998) The stability of phase D at high pressure and temperature. *J. Geophys. Res.* **103**, 7463–7474.
- FUKIZAWA A. (1982) Direct determinations of phase equilibria of geophysically important materials under high pressures and high temperature using in-situ X-ray diffraction method. Ph.D. Thesis, Univ. of Tokyo, Tokyo.
- FURNISH M. D. and BASSETT W. A. (1983) Investigation of the mechanism of the olivine-spinel transition in fayalite by synchrotron radiation. *J. Geophys. Res.* **88**, 10333–10341.
- GASPARIK T. (1989) Transformation of enstatite-diopside-jadeite pyroxenes to garnet, *Contrib. Mineral. Petrol.* **102**, 389–405.
- GASPARIK T. (1990) Phase relations in the transition zone. *J. Geophys. Res.* **95**, 15751–15769.
- GASPARIK T. (1992) Melting experiments on the enstatite-pyrope joint at 80–152 kbar. *J. Geophys. Res.* **97**, 15181–15188.
- GASPARIK T., WOLF K., and SMITH C. M. (1994) Experimental determination of phase relations in the CaSiO<sub>3</sub> system from 8 to 15 GPa. *Am. Mineral.* **79**, 1219–1222.
- GURNEY J. J. (1989) Diamonds. In *Kimberlites and Related Rocks* (eds. J. ROSS *et al.*), pp. 935–965, Geol. Soc. Australia.
- HARLEY S. (1984) An experimental study of the partitioning of Fe and Mg between garnet and orthopyroxene. *Contrib. Miner. Petrol.* **86**, 359–373.
- HAZEN R. M., DOWNS R. T., FINGER L. W., CONRAD P. G., and GASPARIK T. (1994) Crystal chemistry of Ca-bearing majorite. *Am. Mineral.* **79**, 581–584.
- HERZBERG C. and ZHANG J. (1996) Melting experiments on anhydrous peridotite KLB-1: Compositions of magmas in the upper mantle and transition zone. *J. Geophys. Res.* **101**, 8271–8295.
- HIROSE K., FEI Y., MAO Y., and MAO H. K. (1999) The fate of subducted basaltic crust in the Earth's lower mantle. *Nature* **397**, 53–56.
- INOUE K. (1975) Development of high temperature and high pressure x-ray diffraction apparatus with energy dispersive technique and its geophysical applications. Ph.D. thesis, Tokyo Univ., Tokyo.
- IRIFUNE T. (1987) An experimental investigation of the pyroxene-garnet transformation in a pyrolite composition and its bearing on the constitution of the mantle. *Phys. Earth Planet. Inter.* **45**, 324–336.
- IRIFUNE T. and RINGWOOD A. E. (1987a) Phase transformations in a harzburgite composition to 26 GPa: implications for dynamical behaviour of the subducting slab. *Earth Planet. Sci. Lett.* **86**, 365–376.
- IRIFUNE T. and RINGWOOD A. E. (1987b) Phase transformations in primitive MORB and pyrolite compositions to 25 GPa and some geophysical implications. In *High Pressure Research in Mineral Physics* (eds. M. H. MANGHNANI and Y. SYONO), pp. 231–242, American Geophysical Union, Washington, DC.
- IRIFUNE T. and RINGWOOD A. E. (1993) Phase transformations in subducted oceanic crust and buoyancy relationships at depths of 600–800 km in the mantle. *Earth Planet. Sci. Lett.* **117**, 101–110.
- IRIFUNE T. and ISSHIKI M. (1998) Iron partitioning in a pyrolite mantle and the nature of the 410-km seismic discontinuity. *Nature* **392**, 702–705.
- IRIFUNE T., FUJINO K., and OHTANI E. (1991) A new high-pressure form of MgAl<sub>2</sub>O<sub>4</sub>. *Nature* **349**, 409–411.
- IRIFUNE T., KOIZUMI T., and ANDO J. (1996) An experimental study of the garnet-perovskite transformation in the system MgSiO<sub>3</sub>-Mg<sub>3</sub>Al<sub>2</sub>Si<sub>3</sub>O<sub>12</sub>. *Phys. Earth Planet. Inter.* **96**, 147–157.
- IRIFUNE T., SUSAKI J., YAGI T., and SAWAMOTO H. (1989) Phase transformations in diopside CaMgSi<sub>2</sub>O<sub>6</sub> at pressures up to 25 GPa. *Geophys. Res. Lett.* **16**, 187–190.
- ITA J. and STIXRUDE L. (1992) Petrology, elasticity, and composition of the mantle transition zone. *J. Geophys. Res.* **97**, 6849–6866.
- ITO E. and KATSURA T. (1992) Melting of ferromagnesian silicates under the lower mantle conditions. In *High-Pressure Research: Application to Earth and Planetary Sciences* (eds. Y. SYONO and M. H. MANGHNANI), pp. 315–322, American Geophysical Union, Washington, DC.
- ITO E. and TAKAHASHI E. (1989) Postspinel transformations in the system Mg<sub>2</sub>SiO<sub>4</sub>-Fe<sub>2</sub>SiO<sub>4</sub> and some geophysical implications. *J. Geophys. Res.* **94**, 10,637–10,646.
- ITO E. and YAMADA H. (1982) Stability relations of silicate spinel ilmenites and perovskites. In *High-Pressure Research in Geophysics* (eds. S. AKIMOTO and M. H. MANGHNANI), pp. 405–419, Center for Academic Publishing of Japan, Tokyo.
- ITO E., KUBO A., KATSURA T., AKAOGI M., and FUJITA T. (1998) High-pressure transformation of pyrope (Mg<sub>3</sub>Al<sub>2</sub>Si<sub>3</sub>O<sub>12</sub>) in a sintered diamond cubic anvil assembly. *Geophys. Res. Lett.* **25**, 821–824.
- JACKSON I. (1976) Melting of the silica isotopes SiO<sub>2</sub>, BeF<sub>2</sub> and GeO<sub>2</sub> at elevated pressures. *Phys. Earth Planet. Inter.* **13**, 218–231.
- KANZAKI M. (1987) Ultrahigh-pressure phase relations in the system Mg<sub>4</sub>Si<sub>4</sub>O<sub>12</sub>-Mg<sub>3</sub>Al<sub>2</sub>Si<sub>3</sub>O<sub>12</sub>. *Phys. Earth Planet. Inter.* **49**, 168–175.
- KANZAKI M. (1990) Melting of silica up to 7 GPa. *J. Am. Ceram. Soc.* **73**, 3706–3707.
- KATO T. (1986) Stability relation of (Mg,Fe)SiO<sub>3</sub> garnets,

- major constituents in the Earth's interior. *Earth Planet. Sci. Lett.* **69**, 399–408.
- KATSURA T. and ITO E. (1989) The system  $\text{Mg}_2\text{SiO}_4\text{-Fe}_2\text{SiO}_4$  at high pressures and temperatures: precise determination of stabilities of olivine, modified spinel and spinel. *J. Geophys. Res.* **94**, 15,663–15,670.
- KATSURA T., UEDA A., ITO E., and MOROOKA K. (1998) Post-spinel transition in  $\text{Fe}_2\text{SiO}_4$ . In *Properties of Earth and Planetary Materials at High Pressure and Temperature* (eds. M. H. MANGHNANI and T. YAGI), pp. 435–440, American Geophysical Union, Washington, DC.
- KAWADA K. (1977) System  $\text{Mg}_2\text{SiO}_4\text{-Fe}_2\text{SiO}_4$  at high pressures and temperatures and the earth's interior. Ph.D. thesis, Univ. of Tokyo, Tokyo.
- KINGMA K. J., COHEN R. E., HEMLEY R. J., and MAO H. K. (1995) Transformation of stishovite to a denser phase at lower-mantle pressures. *Nature* **374**, 243–245.
- KITAHARA S. and KENNEDY G. C. (1964) The quartz-coesite transition. *J. Geophys. Res.* **69**, 5395–5400.
- LEE H. Y. and GANGULY J. (1988) Equilibrium compositions of coexisting garnet and orthopyroxene: Experimental determinations in the system  $\text{FeO-MgO-Al}_2\text{O}_3\text{-SiO}_2$ , and applications. *J. Petrol.* **29**, 93–113.
- LI B., LIEBERMANN R. C., and WEIDNER D. J. (1998) Elastic moduli of wadsleyite ( $\beta\text{-Mg}_2\text{SiO}_4$ ) to 7 gigapascals and 873 Kelvin. *Science* **281**, 675–677.
- LIU J. G. and ZHANG R. Y. (1996) Occurrence of intergranular coesite in Sulu ultrahigh-P rocks from China: Implications for fluid activity during exhumation. *Am. Mineral.* **81**, 1217–1221.
- LIU L. G. (1974) Silicate perovskite from phase transformations of pyrope-garnet at high pressure and temperature. *Geophys. Res. Lett.* **1**, 277–280.
- LIU L. G. (1975) Post-oxide phases of forsterite and enstatite. *Geophys. Res. Lett.* **2**, 417–419.
- LIU L. G. (1976) Orthorhombic perovskite phases observed in olivine, pyroxene and garnet at high pressures and temperatures. *Phys. Earth Planet. Inter.* **11**, 289–298.
- LIU L. G. (1977) High pressure  $\text{NaAlSi}_3\text{O}_8$ : The first silicate calcium ferrite isotype. *Geophys. Res. Lett.* **4**, 183–186.
- LIU J., TOPOR L., ZHANG J., NAVROTSKY A., and LIEBERMANN R. C. (1996) Calorimetric study of the coesite-stishovite transformation and calculation of the phase boundary. *Phys. Chem. Minerals* **23**, 11–16.
- MACGREGOR I. D. (1974) The system  $\text{MgO-Al}_2\text{O}_3\text{-SiO}_2$ : Solubility of  $\text{Al}_2\text{O}_3$  in enstatite for spinel and garnet peridotite compositions. *Am. Mineral.* **59**, 110–119.
- MAO H. K., SHEN G., and HEMLEY R. J. (1997) Multivariable dependence of Fe-Mg partitioning in the lower mantle. *Science* **278**, 2098–2100.
- MAO H. K., SHEN G., HEMLEY R. J., and DUFFY T. S. (1998) X ray diffraction with a double hot-plate laser-heated diamond cell. In *Properties of Earth and Planetary Materials at High Pressure and Temperature* (eds. M. H. MANGHNANI and T. YAGI), pp. 27–33, American Geophysical Union, Washington, DC.
- MEYER H. O. A. (1987) Inclusions in diamonds. In *Mantle Xenoliths* (ed. P. H. NIXON), pp. 501–522, John Wiley & Sons.
- MEYER H. O. A., MILLEDGE H. J., and SUTHERLAND F. L. (1995) Unusual diamonds and unique inclusions from New South Wales, Australia. *Extended Abstract, 6th International Kimberlite Conf.*, 379–381.
- MIRWALD P. W., GETTING I. C., and KENNEDY G. C. (1975) Low-friction cell for piston-cylinder high-pressure apparatus. *J. Geophys. Res.* **80**, 1519–1525.
- MIRWALD P. W. and MASSONNE H. J. (1980) The low-high quartz and quartz-coesite transition to 40 kbar between 600° and 1600°C and some reconnaissance data on the effect of  $\text{NaAlO}_2$  component on the low quartz-coesite transition. *J. Geophys. Res.* **85**, 6983–6990.
- MICHAEL P. J. and BONATTI E. (1985) Peridotite composition from the North Atlantic: regional and tectonic variations and implication for partial melting. *Earth Planet. Sci. Lett.* **73**, 91–104.
- MORISHIMA H., KATO T., SUTO M., OHTANI E., URAKAWA S., UTSUMI W., SHIMOMURA O., and KIKEGAWA T. (1994) The phase boundary between  $\alpha$ - and  $\beta$ - $\text{Mg}_2\text{SiO}_4$  determined by in situ X-ray observation. *Science* **265**, 1202–1203.
- NIXON P. H. and BOYD F. R. (1973) Petrogenesis of the granular and sheared ultrabasic nodule suite in kimberlite. In *Lesotho Kimberlites* (ed. P. H. NIXON), pp. 48–56, Lesotho National Development Corp., Lesotho.
- OHTANI E. (1979) Melting relation of  $\text{Fe}_2\text{SiO}_4$  up to 200 kbar. *J. Phys. Earth* **27**, 189–208.
- OHTANI E., KAGAWA N., and FUJINO K. (1991) Stability of majorite ( $\text{Mg,FeSiO}_3$ ) at high pressures and 1800°C. *Earth Planet. Sci. Lett.* **102**, 158–166.
- PACALO R. E. G. and GASPARIK T. (1990) Reversals of the orthoenstatite-clinoenstatite transition at high pressures and high temperatures. *J. Geophys. Res.* **95**, 15853–15858.
- PRESNALL D. C. and GASPARIK T. (1990) Melting of enstatite ( $\text{MgSiO}_3$ ) from 10 to 16.5 GPa and implication for the origin of the mantle. *J. Geophys. Res.* **95**, 15771–15777.
- PRESNALL D. C. and WALTER M. J. (1993) Melting of forsterite,  $\text{Mg}_2\text{SiO}_4$ , from 9.7 to 16.5 GPa. *J. Geophys. Res.* **98**, 19777–19783.
- RINGWOOD A. E. (1958) Constitution of the mantle, III. Consequences of the olivine-spinel transition. *Geochim. Cosmochim. Acta* **15**, 195–212.
- RINGWOOD A. E. (1962a) A model for the upper mantle. *J. Geophys. Res.* **67**, 857–866.
- RINGWOOD A. E. (1962b) Mineralogical constitution of the deep mantle. *J. Geophys. Res.* **67**, 4005–4010.
- RINGWOOD A. E. (1966) Mineralogy of the mantle. In *Advances in Earth Science* (ed. P. M. HURLEY), pp. 357–398, MIT Press, Cambridge.
- RINGWOOD A. E. (1979) *Origin of the Earth and Moon*. Springer-Verlag, New York.
- RINGWOOD A. E. and MAJOR A. (1966) Synthesis of  $\text{Mg}_2\text{SiO}_4\text{-Fe}_2\text{SiO}_4$  solid solutions. *Earth Planet. Sci. Lett.* **1**, 241–245.
- RINGWOOD A. E. and MAJOR A. (1970) The system  $\text{Mg}_2\text{SiO}_4\text{-Fe}_2\text{SiO}_4$  at pressures and temperatures. *Phys. Earth Planet. Inter.* **3**, 89–108.
- RINGWOOD A. E. and SEABROOK M. (1962) Olivine-spinel equilibria at high pressure in the system  $\text{Ni}_2\text{GeO}_4\text{-Mg}_2\text{SiO}_4$ . *J. Geophys. Res.* **67**, 1975–1985.
- SAWAMOTO H. (1986) Single crystal growth of the modified spinel ( $\beta$ ) and spinel ( $\gamma$ ) phases of  $(\text{Mg,Fe})_2\text{SiO}_4$  and some geophysical implications. *Phys. Chem. Minerals* **13**, 1–10.
- SAWAMOTO H. (1987) Phase diagram of  $\text{MgSiO}_3$  at pressures up to 24 GPa and temperatures up to 2200 K: phase stability and properties of tetragonal garnet. In *High-Pressure Research in Mineral Physics* (eds. M. H. MANGHNANI and Y. SYONO), pp. 209–219, Terra Publications, Tokyo.
- SHEN G., MAO H. K., and HEMLEY R. J. (1996) Laser-heated diamond anvil cell technique: Double-sided heating with

- multimode Nd:YAG laser. *Proc. Advanced Materials '96*, 149–152.
- SHIMIZU N. (1974) Rare earth elements (REE) in garnets and clinopyroxenes from garnet lherzolite nodule in kimberlite. *Carnegie Inst. Washington Yearb.* **73**, 954–961.
- SOBOLEV N. V., YEFIMOVA E. S., and KOPTIL V. I. (1998) Crystalline inclusions in diamonds in the Northeast of the Yakutian diamondiferous province. *Extended Abstract, 7th International Kimberlite Conf.*, 832–834.
- SOBOLEV N. V., YEFIMOVA E. S., REIMERS L. F., ZAKHARCHENKO O. D., MAKHIN A. I., and USOVA L. V. (1995) Arkhangelsk diamond inclusions. *Extended Abstract, 6th International Kimberlite Conf.*, 558–560.
- STISHOV S. M. and POPOVA S. V. (1961) A new dense modification of silica. *Geochemistry (USSR)* **10**, 923–926.
- STIXRUDE L. (1997) Structure and sharpness of phase transitions and mantle discontinuities. *J. Geophys. Res.* **102**, 14835–14852.
- SUTO K. (1972) Phase transitions of pure  $Mg_2SiO_4$  into a spinel structure under high pressures and temperatures. *J. Phys. Earth* **20**, 225–243.
- SUTO K. (1977) Phase relations of pure  $Mg_2SiO_4$  up to 200 kilobars. In *High-Pressure Research: Application to Geophysics* (eds. M. H. MANGHNANI and S. AKIMOTO), pp. 365–371, Academic Press, New York.
- SUNG C. M. and BURNS R. G. (1976) Kinetics of high-pressure phase transformations: implications to the evolution of the olivine-spinel transition in the downgoing lithosphere and its consequences on the dynamics of the mantle. *Tectonophysics* **31**, 1–32.
- SUN S. (1982) Chemical composition and origin of the Earth's primitive mantle. *Geochim. Cosmochim. Acta* **16**, 179–192.
- TAKAHASHI E. (1986) Melting of a dry peridotite KLB-1 up to 14 GPa: Implications on the origin of peridotitic upper mantle. *J. Geophys. Res.* **91**, 9367–9382.
- TAKAHASHI E. and ITO E. (1987) Mineralogy of mantle peridotite along a model geotherm up to 700 km depth. In *High Pressure Research in Mineral Physics* (eds. M. H. MANGHNANI and Y. SYONO), pp. 427–438, American Geophysical Union, Washington, DC.
- TETER D. M., HEMLEY R. J., KRESSE G., and HAFNER J. (1996) High pressure polymorphism in silica. *Phys. Rev. Lett.* **80**, 2145–2148.
- TSE J. S. and KLUG D. D. (1992) Novel high pressure phase of silica. *Phys. Rev. Lett.* **69**, 3647–3649.
- TSUCHIDA Y. and YAGI T. (1989) A new, post-stishovite high-pressure polymorph of silica. *Nature* **340**, 217–220.
- WOOD B. J. (1974) The solubility of alumina in orthopyroxene coexisting with garnet. *Contrib. Mineral. Petrol.* **46**, 1–15.
- WOOD B. J. and BANNO S. (1973) Garnet-orthopyroxene and orthopyroxene-clinopyroxene relationships in simple and complex system. *Contrib. Mineral. Petrol.* **42**, 109–124.
- YAGI T. and AKIMOTO S. (1976) Direct determination of coesite-stishovite transition by in-situ X-ray measurements. *Tectonophysics* **35**, 259–270.
- YAGI T., BELL P. M., and MAO H. K. (1979) Phase relations in the system  $MgO-FeO-SiO_2$  between 150 and 700 kbar at 1000°C. *Carnegie Inst. Washington Yearb.* **78**, 614–616.
- YAGI T., AKAOGI M., SHIMOMURA O., SUZUKI T., and AKIMOTO S. (1987) In situ observation of the olivine-spinel phase transformation in  $Fe_2SiO_4$  using synchrotron radiation. *J. Geophys. Res.* **92**, 6207–6213.
- YASUDA A., FUJII T., and KURITA K. (1994) Melting phase relations of an anhydrous mid-ocean ridge basalt from 3 to 20 GPa: implications for the behavior of subducted oceanic crust in the mantle. *J. Geophys. Res.* **99**, 9401–9414.
- YUSA H., AKAOGI M., and ITO E. (1993) Calorimetric study of  $MgSiO_3$  garnet and pyroxene: heat capacities, transition enthalpies, and equilibrium phase relations in  $Mg-SiO_3$  at high pressures and temperatures. *J. Geophys. Res.* **98**, 6453–6460.
- ZHA C., DUFFY T. S., MAO H. K., DOWNS R. T., HEMLEY R. J., and WEIDNER D. J. (1997) Single-crystal elasticity of  $\beta-Mg_2SiO_4$  to the pressure of the 410 km seismic discontinuity in the Earth's mantle. *Earth Planet. Sci. Lett.* **147**, E9–E15.
- ZHA C., DUFFY T. S., MAO H. K., DOWNS R. T., HEMLEY R. J., and WEIDNER D. J. (1998) Single-crystal elasticity of the  $\alpha$  and  $\beta$  polymorphs of  $\beta-Mg_2SiO_4$  at high pressure. In *Properties of Earth and Planetary Materials at High Pressure and Temperature* (eds. M. H. MANGHNANI and T. YAGI) pp. 200–208, American Geophysical Union, Washington, DC.
- ZHANG J. and HERZBERG C. (1994) Melting experiments on anhydrous peridotite KLB-1 from 5.0 to 22.5 GPa. *J. Geophys. Res.* **99**, 17729–17742.
- ZHANG J., LIEBERMANN R. C., GASPARIK T., HERZBERG C. T., and FEI Y. (1993) Melting and subsolidus relations of  $SiO_2$  at 9 to 14 GPa. *J. Geophys. Res.* **98**, 19,785–19,793.
- ZHANG J., LI B., UTSUMI W., and LIEBERMANN R. C. (1996) In situ X-ray observations of the coesite-stishovite transition: reversed phase boundary and kinetics. *Phys. Chem. Minerals* **23**, 1–10.
- ZHANG R. Y., LIU J. G., and TSAI C. H. (1996) Petrogeneses of a high-temperature metamorphic belt: a new tectonic interpretation for the north Dabieshan, Central China. *J. Meta. Geol.* **14**, 319–333.

